# Progress in Twin Screw Extrusion Technology Focused on Compounding

Tadamoto Sakai

Plastics Age, **66** (6), p42 (2020), Plastics Age, **66** (7), p67 (2020), Plastics Age, **66** (8), p68 (2020),

## Summary

Compounding technology using a twin screw extruder is playing especially important roles both in development and in production for various functional polymer composites and polymer-alloys having nano-scale morphology. In this review developments in recent technical innovation in the polymer processing fields related to compounding were outlined, introducing several practical examples.

## Forward

A plastic product is rapidly growing toward various applications used for high functionality in the agricultural fields such as multi-film, in the industrial fields such as package and car parts, in the electronic/optical fields, in the energy related fields such as solar battery parts, and moreover in the medical and welfare fields.[1,2] Two kinds of major trends are significantly progressing these days; one is toward efficient production technology to raise higher productivity and better energy saving, and the other is toward new plastic products with advanced functions or highly additional values. Twin screw extrusion technology has been supporting to these trends mentioned above by remarkable developments in mechanical design, theoretical analyses on extrusion characteristics and compounding techniques for nano-fillers such as carbon nano-tube and polymer alloys with the nano-level morphology. In this review recent technical innovations were introduced in the compounding fields related to a twin screw extruder.

## 1. Developments in twin screw extruder design technology

### 1.1 Changes of screw and cylinder structure of a twin screw extruder

An intermeshed co-rotational twin screw extruder consists of the modular structure of screw elements and barrel units to apply flexibly to various kinds of plastic material and sub-material compounding.

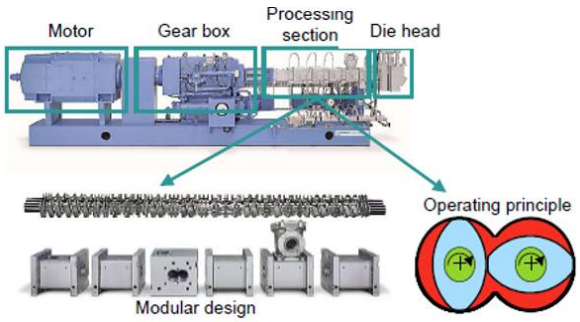


Fig. 1. Basic structure of a co-rotation intermeshed twin screw extruder

Figure 2 shows historical transition on screw channel depth, screw mixing element design and screw driving torque of a twin screw extruder. From Figure 2 we can easily learn the drastic change in screw channel depth, rotational speed, driving torque and mixing element design since the basic concept of a

twin screw extruder was established around 1930's [3].

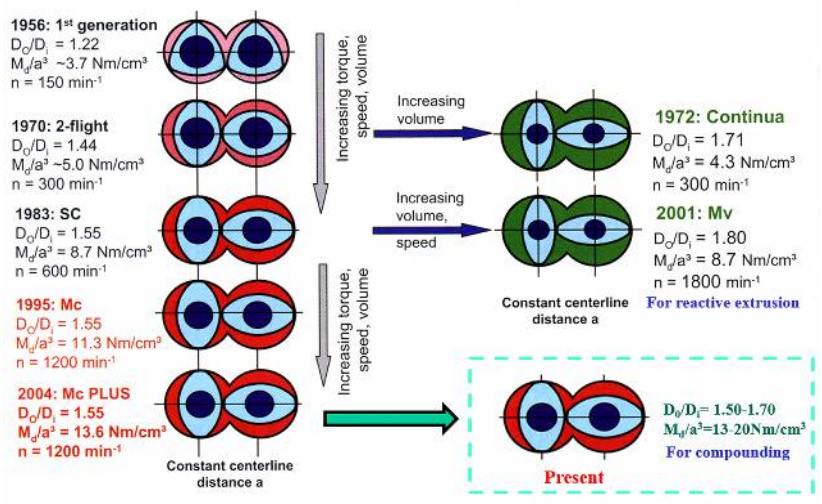


Fig. 2. Change of the structure of a twin screw extruder focussed on screw design and driving force

### (1) Increase of screw channel depth (*Do/Di*)

A screw channel depth ratio (screw outer diameter/screw inner diameter : *Do/Di*) was about 1.2 at the early generation of a twin screw extruder, but the depth ratio has been gradually increased to 1.5-1.8. The popular shape of a kneading disc element was changed from three lobe type to two lobe one. Therefore, the following improvements have been accomplished, such as the increase of conveying volume per screw rotation, the increase of residence time, the decrease of energy consumption per throughput and furthermore lower polymer temperature operations for efficient mixing and kneading.

### (2) Increase of screw rotational speed

In the early stage screw rotational speed of a twin screw extruder was in the range of 100-200 rpm, but nowadays it has attained to 600-1500 rpm, showing speed-up tendency year after year. The increase of screw speed allows improvement in throughput, as well as better mixing and kneading capability under high shearing operations. As a special example, high screw speed as much as 2500 rpm is sometimes applied to control the morphology formation of polymer alloys.

### (3) Increase of total screw length (*L/D*)

The demand for long screw length (*L/D*) has been increased because of diversified mixing and kneading operations, such as multi-stage feeding and multi-stage devolatilization, to obtain advanced polymer alloys and composites in recent years. Moreover, the screw length of *L/D* is closely related to the length of residence time to promote mixing and kneading actions (distributive mixing) and chemical reactions under compounding operations, that is, longer *L/D* leads to longer residence time. Today a twin screw extruder is generally used with *L/D* of 30-60, but for special polymer-alloy compounding, *L/D* is attained around 100[4].

### (4) Increase of torque density for screw driving

To obtain higher throughput and better mixing operations using a twin screw extruder, the extruder has been continuously required to increase driving power, i.e., higher screw torque. In the early generation of 1960's, the screw torque density was only 3-5 N·m/cm$^3$, but at present the screw torque density has reached the level of 15-20 N·m/cm$^3$. Higher screw torque density means higher screw torque, which is necessary for compounding. Higher screw torque enables to better mixing and kneading operations and larger throughput. And furthermore, it means that a polymer with high viscosity can be applied for compounding at lower polymer temperature (i.e., higher melt-viscosity and less thermal degradation) while a conventional twin screw extruder with lower screw torque is not applicable.

Figure 2 shows the relationship between screw torque density and applicable operational conditions[5]. This Figure shows that throughput can be raised from 400 kg/h to 660 kg/h at screw speed of 700 rpm, if the operating line ($M_d$= 69%) of high screw torque density is shifted from the operating line ($M_d$= 50%). Moreover, better mixing and kneading operation becomes possible not only with higher throughput from 660 kg/h to 930 kg/h, but also at lower polymer temperature from 290$^0$C to 275$^0$C if the operation along the operating line ($M_d$ = 90%) is applied. In conclusion, it is clearly suggested that improvements in efficient compounding both for the creation of advanced functions and for the reduction in thermal deterioration of polymers are accelerating, if a twin screw extruder with higher screw torque density is used.

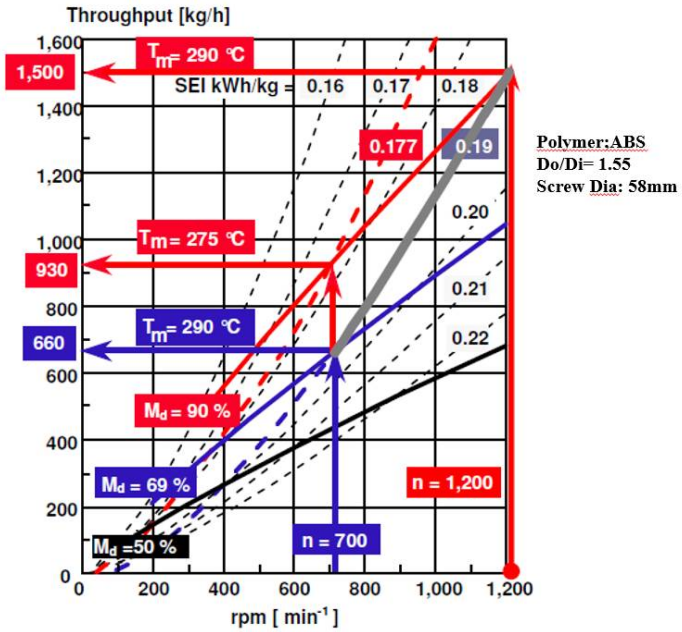


Fig. 3. Relationship between productivity improvement and screw driving torque.

## 2. Developments in mixing and kneading technology

Mixing and kneading actions in a screw flow channel for a molten-polymer are classified into the following categories[6].

(1) Shear mixing under shearing flow

(2) Elongational mixing under elongational flow

(3) Diffusion mixing

(4) Chaotic mixing

In these mixing processes shear mixing in the flow fields plays the most important role in the determination of mixing and kneading performance in a twin screw extruder, and this is classified into two kinds of mixing, *i.e.,* distributive mixing and dispersive one. Distributive mixing is evaluated by the level of shear strain, which is product of shear rate and residence time. In contrast, dispersive mixing is evaluated by the level of shear stress, which is product of shear rate and melt-viscosity of a molten polymer. That is, it is important to make residence time longer for distributive mixing. But residence time is irrelevant in dispersive mixing and it is more effective to obtain better dispersive mixing when applied to lower polymer temperature to utilize the increase of melt-viscosity. Figure 4 clearly explains the difference between distributive mixing and dispersive mixing in the extruder flow channel. It is strongly required strengthening of dispersive mixing to reduce the domain size and the number of aggregates in polymer-blending or inorganic filler compounding. In distributive mixing, efficient mixing action can be carried out by repeating cyclic movements such as multi-stage folding actions and/or multi-layering actions for each polymer component.

Lately elongational mixing induced by stretching actions in the flow field attracts attention as more effective mixing process with better energy efficiency, because elongational mixing is suitable for multi-component polymer blending or inorganic nano-filler compounding. The elongational mixing will be discussed later at paragraph 2.3.

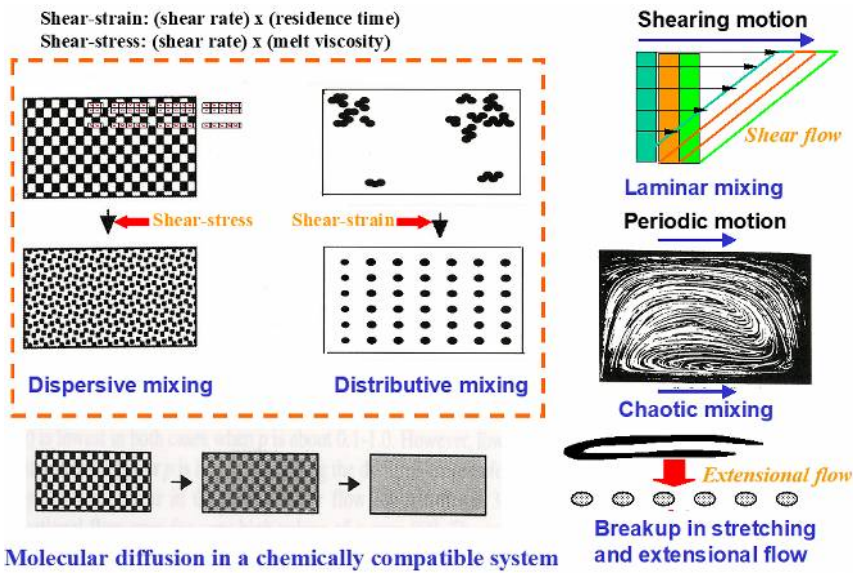


Fig. 4. Various mixing/kneading models generated in the screw channel flow.

### 2.1. Operational factors used for compounding.

There are much greater number of operational factors of a twin screw extruder and further each factor is deeply connecting, when compared with those of a single screw extruder. Figure 5 shows various mixing stages related to twin screw compounding (left side) and operational factors (right side) to control these processes, respectively. As shown in Figure 5, it is indispensable how to control and how to optimize these operational factors in compounding. In compounding using a twin screw extruder,

screw rotational speed and feeding rate (*i.e.,* throughput) are independent as separated operational factors, while in a single screw extruder it is difficult to control independently screw rotational speed and throughput. It is because the throughput of a single screw extruder is intricately connected to screw rotational speed. Furthermore, in a twin screw extruder, it is possible to supply various raw materials separately from several locations of the extruder as one of compounding techniques, *e.g.*, the prevention of glass fiber breaking-down or the control of the morphology formation in a polymer alloy. Figure 6 shows the difference in each residence time distribution at the corresponding zones in a twin screw extruder[7]. In the melting zone residence time distribution is considerably narrow, but high shear stress is generated. As a result, strong dispersive mixing action is brought about in this zone. In contrast, in the mixing and kneading zone wider residence time distribution and higher distributive mixing action can be generally applied. Therefore, in actual compounding operations it is necessary to optimize the combination of screw elements for efficient mixing actions and for suitable residence time profiles at each zone.

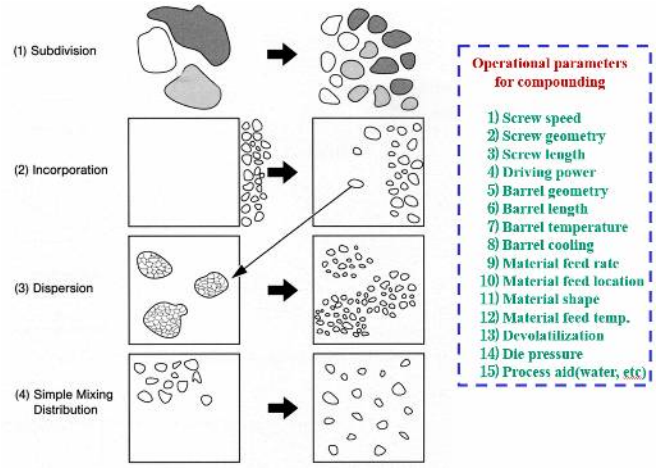


Fig. 5. Mixing and kneading processes and operational factors in a twin screw extruder

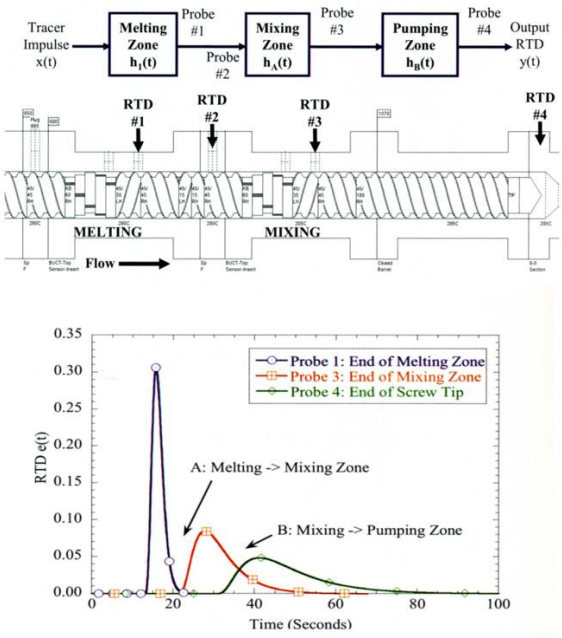


Fig. 6. Residence time distributions at each zone of a twin screw extruder

### 2.2. Shear mixing.

When cohesion force among filler particles such as carbon black and nano-silica is extraordinarily strong, it is necessary to apply strenuous shear stress for dispersion. Figure 7 shows the relationship between shear stress applied and resulting dispersion of carbon black as an experimental example. The author reported that the dispersion of various inorganic fillers was improved when large shear stress was loaded[8]. In general, shear stress plays an important role in dispersing various inorganic fillers, but in other cases the dispersion of fillers is dominated not only by shear stress, but also by shear strain, when evaluated from the combination of other polymer and various inorganic fillers. As shown in Figure 8, the mixing and kneading effects are dominated by shearing energy (product of shear strain and shear stress), *i.e.,* specific energy *Esp* (energy consumption per throughput)[9].

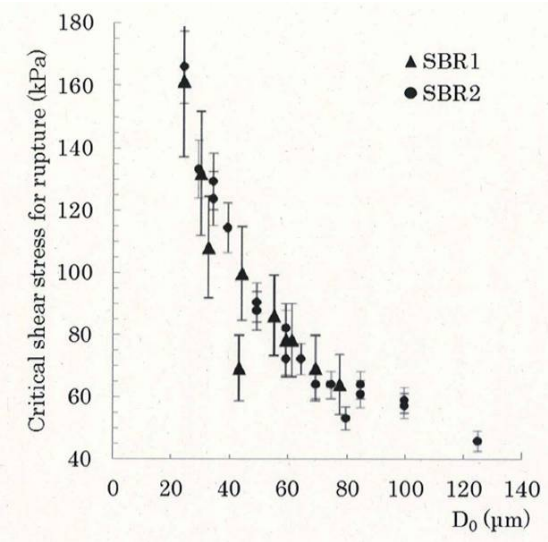


Fig. 7. Critical shear stress to influence carbon black dispersion in SBR.

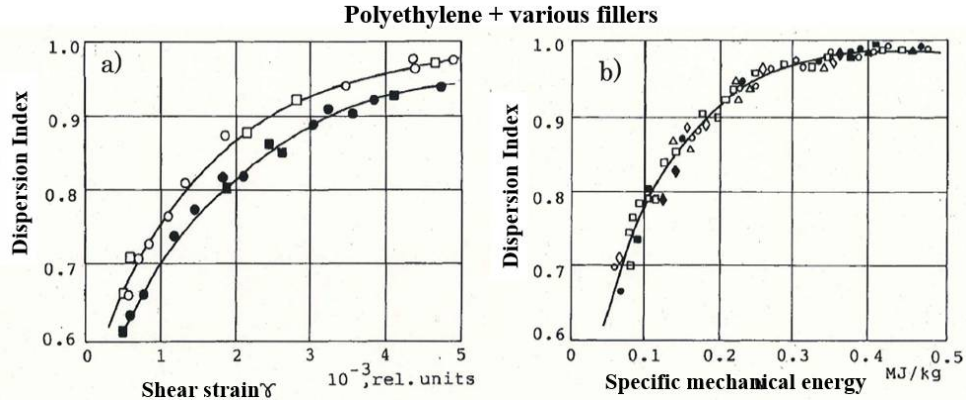


Fig. 8. Effects of shear strain and specific energy on dispersion of various inorganic fillers

### 2.3. Elongational mixing.

Recent years lots of practical research aimed at improvement in mixing and kneading by utilizing elongational flow have been considerably progressing. Figure 9 shows the relationship between

melt-viscosity ratio of a blending components and critical capillary number in the shearing flow field and in the elongational flow field, respectively[10]. An area to be obtainable good mixing conditions exists inside each line in Figure 9 both for shear flow and for elongational flow. Figure 9 clearly shows that good mixing and kneading effects are easily obtained in a polymer blending system with large melt viscosity ratio, when the elongational flow field is formed.

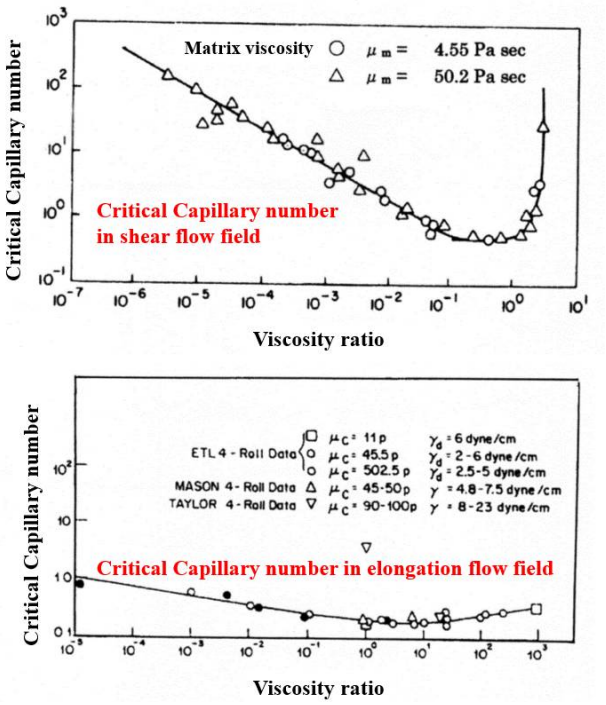


Fig. 9. Relationship between break-up of droplets and Capillary number/viscosity ratio

Figure 10 shows a theoretical computation result carried out by M. Gupta *et al* on the elongational flow in a twin screw extruder. From Figure 10 it is clear the elongational flow is specifically occurred in the area where each tip of two kneading disc elements is intersecting (intermeshing)[11].

Figures 11-12 show experimental research results observed on elongational mixing behavior[12]. Figure 11 shows a system to evaluate elongational mixing continuously generated in the flow passing through a nozzle placed between two pistons. Furthermore, Figure 12 shows the data on consumption energy for mixing in binary polymer blending and how to advance the domain size reduction. Concerning the domain size of a polymer-alloy obtained from this system, it was observed higher quality or better dispersion effect than those from a twin screw extruder, when the elongational mixing action was added. Moreover, from this experiment it was proved that mixing energy obtained from this system was lower than that from a twin screw extruder.

In practical ways, L. Utracki *et al* carried out several experiments on the dispersion acceleration in nano-clay compounding by using a special elongational mixing device, so-called "EFM" (Elongational Flow Mixer). They reported that higher dispersion effect for nano-clay was obtained when EFM device and a single screw extruder was directly combined[13].

| | | | | |
|---|---|---|---|---|
| Shear viscosity | $\eta_0$ | $1.24 \times 10^5$ Pa·s | | |
| | $\lambda$ | 63.3 s | $n$ | 0.401 |
| Elongational viscosity | Planar | | | |
| | $\delta$ | 37.3 | $\lambda_1$ | 2250.0 s |
| | $\lambda_2$ | 46.2 s | $m$ | 0.4 |
| | Axisymmetric | | | |
| | $\delta$ | 0.0 | $\lambda_2$ | 2.18 s |
| | $m$ | 0.349 | | |

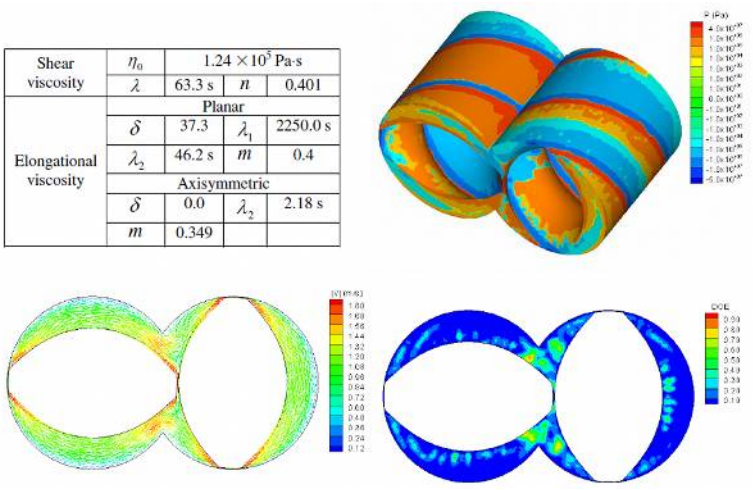

Fig.10. Elongational flow analysis in kneading discs of a twin screw extruder

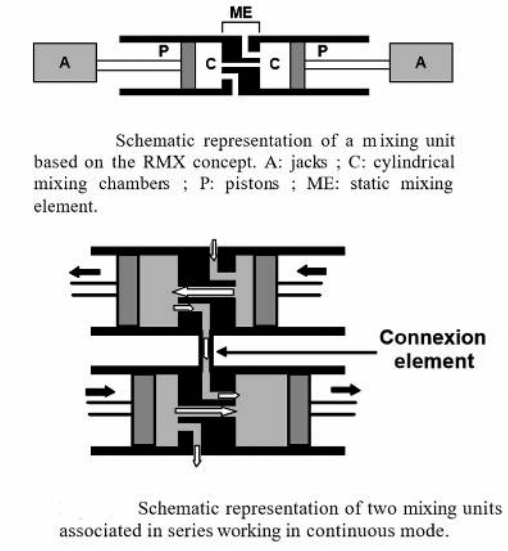


Schematic representation of a mixing unit based on the RMX concept. A: jacks ; C: cylindrical mixing chambers ; P: pistons ; ME: static mixing element.

Schematic representation of two mixing units associated in series working in continuous mode.

Fig.11. A mixer structure to obtain elongational mixing (RMX)

| Sample | $D_N$ (µm) | $D_V$ (µm) | $D_W/D_N$ | $W_M$ kJ/kg |
|---|---|---|---|---|
| PMMA/PS RMX 30 cycles | 0.08 | 0.12 | 1.47 | 380 |
| PMMA/PS Rheomix 600 | 0.24 | 0.45 | 1.89 | 630 |
| PA/PE RMX 15 cycles | 0.23 | 0.97 | 4.15 | 125 |
| PA/PE RMX 30 cycles | 0.24 | 0.74 | 3.05 | 250 |
| PA/PE RMX 90 cycles | 0.2 | 0.58 | 2.86 | 750 |
| PA/PE Twin screw extruder | 0.21 | 0.41 | 1.98 | 1080 |

**Number – and volume average diameters, polydispersity and mixing energy.** (TSE: 30mm, 300rpm, 15kg/h)

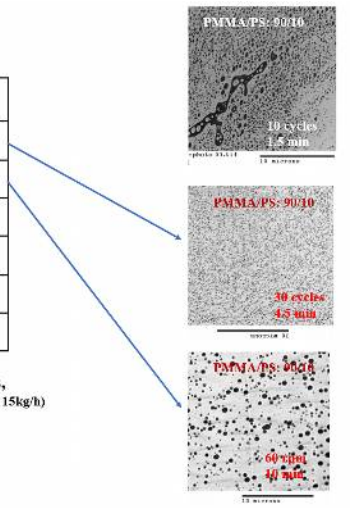


Fig. 12. Mixing behavior comparisons between RMX elongational mixer and twin screw extruder

### 3. Technological developments in assembling ways on screw elements for compounding operations

A lot of complicated mixing screw elements for a twin screw extruder have been developed to use for various compounding operations of polymer-alloys and polymer composites. Several examples are shown in Figure 13. The main feature of these mixing screw elements is the flexibility to obtain divesified screw combinations by selecting a wide variety of the disc thickness and stagger angle. Moreover, in addition with the flexibility in screw combination design, some special developments have been progressing, for example, new screw elements to promote elongational mixing and a specific cylinder with several grooves to aim at synergetic mixing effects between a screw tip and cylinder inner surface with shallow grooves[6,14,15].

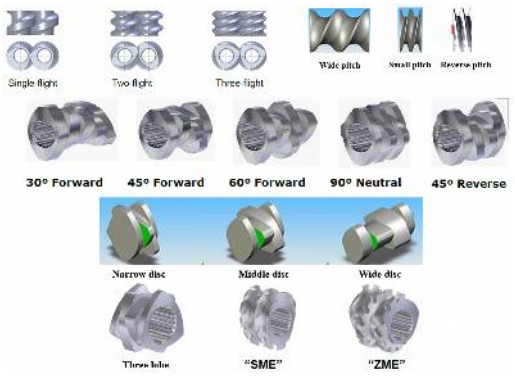


Fig.13. Typical mixing screw elements used for twin screw compounding.

#### 3.1. Relationship between kneading disc width, stagger angle and mixing effects.

For compounding operations, widely-used methods are thickness adjustment of a disc type mixing element and multi-functional combination with different stagger angle. As an example, Figure 14 shows diversified combinations of various kneading disc elements, depending on polymer alloys/composites or operational purposes. Moreover, distinctive extrusion characteristics obtained from different disc combinations are listed in Figure 14. Typically, the combination is applied to thicker (wider) kneading discs for strengthening dispersive mixing. In contrast, the combination of thinner (narrower) kneading discs is applied for aiming at efficient distributive mixing.

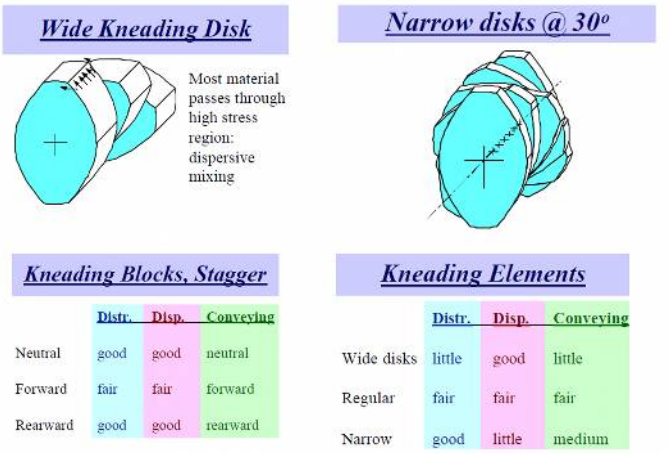


Fig. 14. Combinations of various kneading discs and mixing effects obtained

Moreover, Figure 15 shows the relationship between the degree of distributive mixing obtained experimentally and the combination of different kneading discs. The degree of distributive mixing was evaluated using conversion ratio of a reactive tracer. In this case the degree of distributive mixing is correspondingly high as much as the conversion ratio is high[16]. From Figure 15 it is clear that high distributive mixing effects were otained both from the neutral kneading disc combination (*i.e.,* stagger angle is $90^0$) and from the reverse kneading discs combination (*i.e.,* left-handed stagger), when kneading discs with thin thickness were used. On the contrary, considerably high distributive mixing effect was obtained under small throughput operation, when the kneading discs with right-handed stagger were selected. Furthermore, lower disctributive mixing effects were obtained from the thick kneading discs, when different thickness was compared.

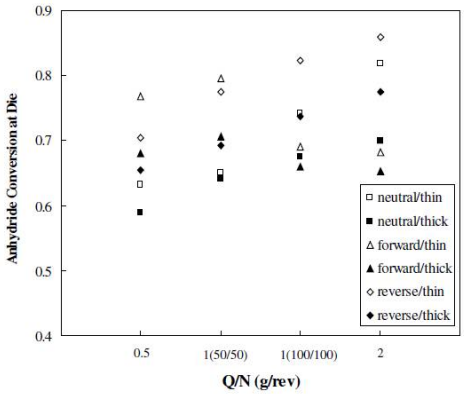


Fig.15. Evaluation of distributive mixing effects from various mixing elements using a reactive tracer

### 3.2. Relationship between various screw elements and mixing/kneading.

For a twin screw extruder, a rotor type screw element is often used in addition to kneading disc type elements. Figures 16-18 show the difference of mixing behavior obtained by theoretical flow analysis and by experiments on right-handed screw elements (ND), kneading disc elements (KD) and moreover rotor type screw element (VCR), respectively[17]. Each screw element was inserted in the mixing zone (*L/D*=4) where molten polymer was completely filled. The experimental results for a mixing and kneading system of low-density polyethylene (LDPE) added magnesium-hydroxide ($Mg(OH)_2$ 30%) were reported as follows; the dispersive mixing effect was increased in order of **KD ≥ VCR > NS** and the distributive mixing effect was increased in order of **VCR > KD > NS.** In contrast, the transportation capability of a molten polymer became better in order of **ND > KD > VCR.**


Figure 16. Combination of various mixing screw elements

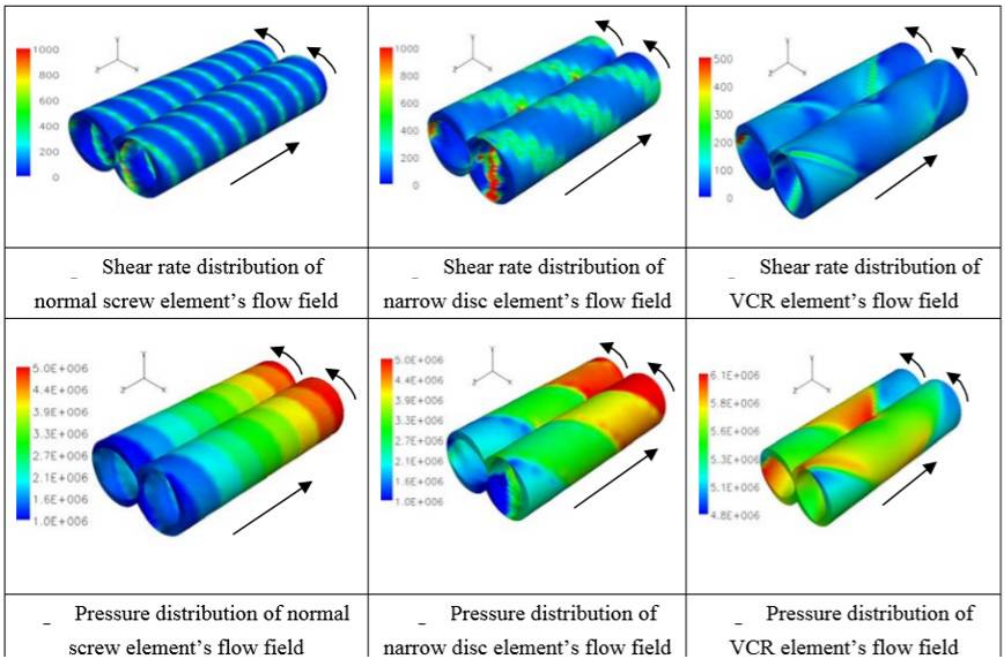


Fig. 17. Characteristic analyses for various mixing screw elements

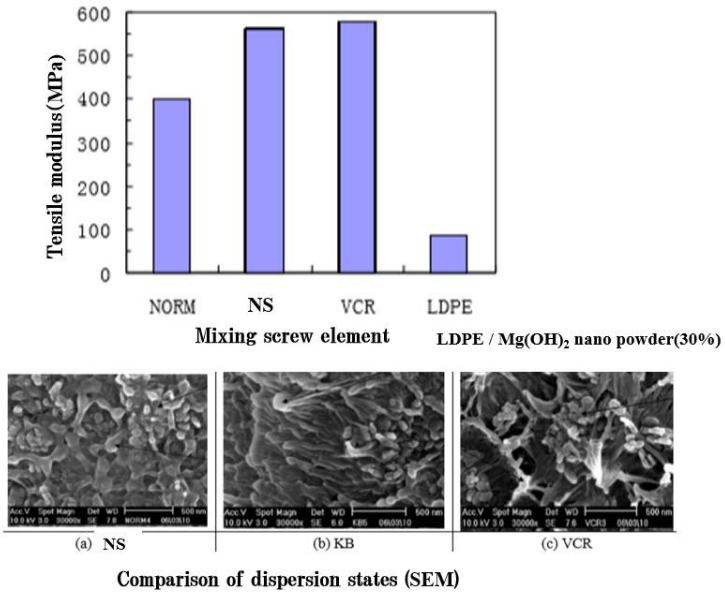


Fig.18. Comparison of mixing and kneading effects of various mixing elements

### 3.3. Relationship between assembling ways of gear type mixing screw elements and mixing effects

A gear type mixing screw element is widely and practically used for the compounding of a typical kneading/mixing system with high viscosity ratio to promote mainly for distributive mixing. Figure 19-20 show the kneading/mixing effects from different assemblining of gear type mixing screw elements[18]. In particular, Figure 20 shows that higher distributive mixing effect was obtained with the gear type mixing screw elements combined at proper interval (bottom in Figure 19), when the screw elements continuously aligned (upper in Figure 19) was compared.

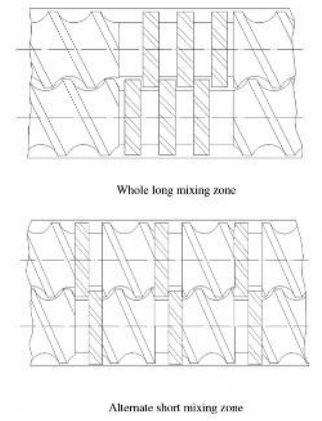


Fig. 19. Two kinds of the arrangement of gear type mixing screw elements

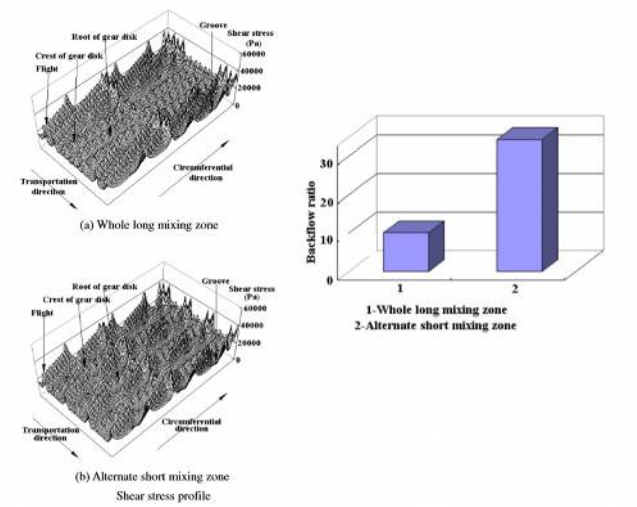


Fig. 20 Difference in mixing behavior from the arrangement of gear type mixing screw elements

### 3.4. Relationship between the combination of various screw elements and shear stress generation.

While theoretical flow analyses have been rapidly progressing, experimental studies to verify the flow behavior in a twin screw extruder have been also increasing.

For an example, Figure 21 shows break-up behavior of special glass beads added as a tracer to measure real stress generation at a mixing zone located in a twin screw extruder[19]. The glass beas can be easily destroyed under constant stress. This Figure shows break-up percentage of glass beads destroyed by a certain level of shear stress. Larger value means that bigger shear stress was generated in the screw flow channel. That is, it is proved experimentally that thick kneading discs is possible to produce bigger shear stress more than thin kneading discs under the same operational conditions such as screw rotational speed and throughput. Moreover, it shows that shear stress to contribute to dispersive mixing becomes larger, as increased either screw rotational speed or throughput. From our experience it is wellknown that thick kneading discs can bring about higher shear stress, *i.e.* excellent dispersive mixing but lower distributive mixing, when compared with thin kneading discs. As shown in Figure 21, the experimental results introduced here are well corresponding to our emprical knowledge.

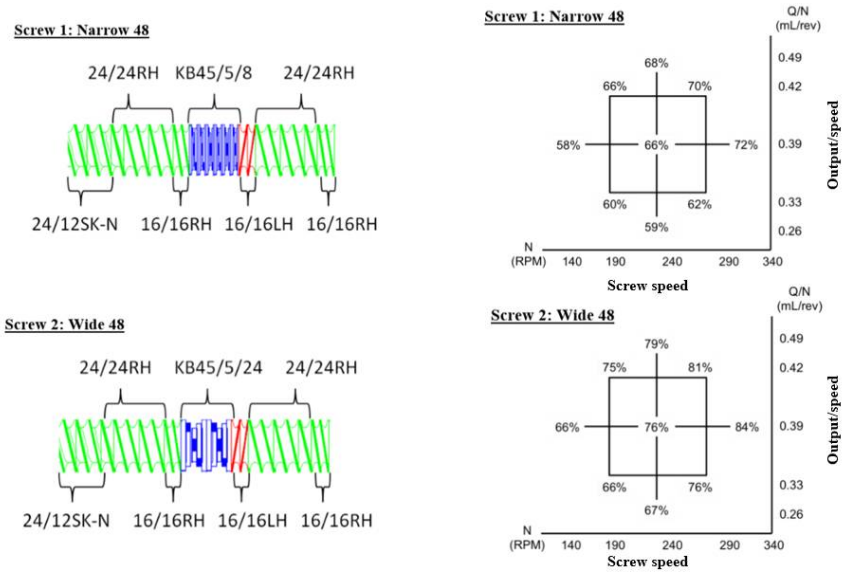


Fig. 21. Relationship between the shape of kneading discs and the fracture of glass beads

### 3.5. Relationship between the combination of twin screw elements and thermal conductivity

In a twin screw extruder, major energy supplied from screw rotation is consumed the melting and mixing of a polymer. Therefore, a molten polymer temperature is mainly dominated by this energy consumption. However, heat conduction through a cylinder are also important to control polymer temperature as one of essential operational factors. Few studies were reported on the relationship between heat transfer coefficient and mixing screw element combinations. Figure 22 shows research results that S. Tenge *et al* verified the influence of various mixing screw elements on heat conduction behavior between a cylinder and molten polymer[20]. It is interesting that heat transfer coefficient was changed dependent on screw element combinations as shown in Figure 22.

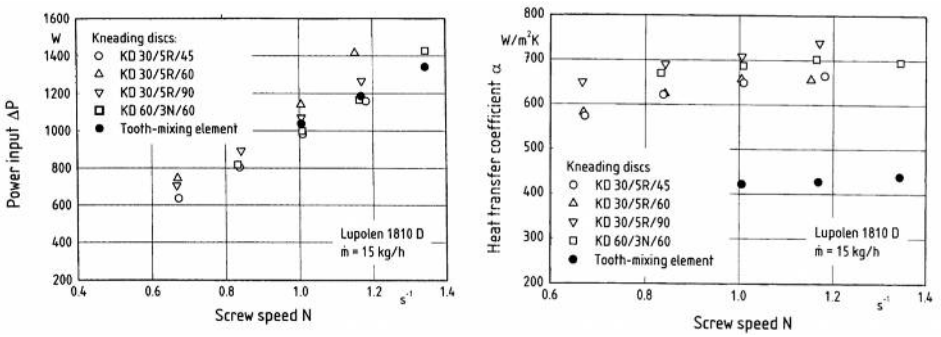


Fi.g. 22. Influence on heat transfer coefficient with different kneading screw elements

## 4. Developments in analysis technology on twin screw compounding

### 4.1. Analyses on morphology evolution of a polymer-alloy in a twin screw extruder

Concerning analyses on the morphology evolution process of a polymer-alloy in a twin screw extruder, several methods were reported, for examples, the use of glass windows inserted on the cylinder of a twin screw extruder to visualize and on-line extraction of a molten polymer-alloy to evaluate mixing/kneading or chemical reaction stages at each zone from sampling nozzles attached along the cylinder[21,22]. In addition to these studies mentioned above, C. Shih *et al* developed a new analysis

method to evaluate inline the behavior on mixing and polymerization reaction by the measurement on local residence time distribution and energy consumption at each zone of a twin screw extruder. This method is called a "pulse-feeding" method. Figure 23 shows an experimental procedure of this method and Figure 24 is the experimental results on an evolution process of a polymer-alloy obtained by this analysis[23,24]. In the reaction system as shown the left side in Figure 24, the morphology evolution of a polymer-alloy was taken place at the mixing and kneading zone after the base polymer was already melted. In contrast, in the reaction system as shown the right side in Figure 24, the morphology evolution of a polymer-alloy was taken place simultaneously together with the melting completion of the base polymer at the melting zone and no futher chemical reaction was detected at the mixing and kneading zone.

As shown in these examples, the pulse-feeding method can use where the morphology evolution of a polymer alloy occures in a twin screw extruder and how the screw elelment combination or operational conditions should be optimized depending on polymerization reactions.

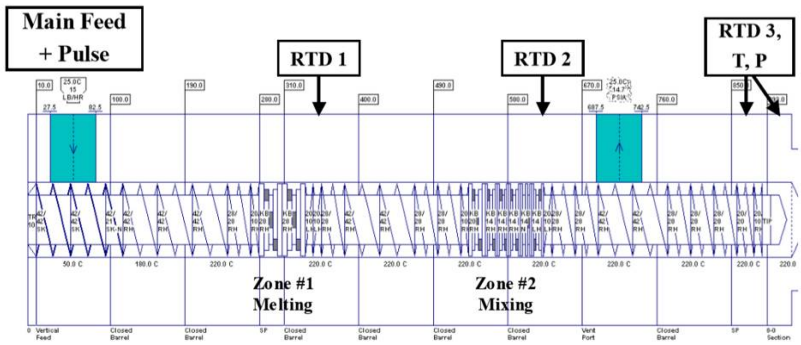


Fig. 23 Experimental setup for measuring local residence time and driving power.

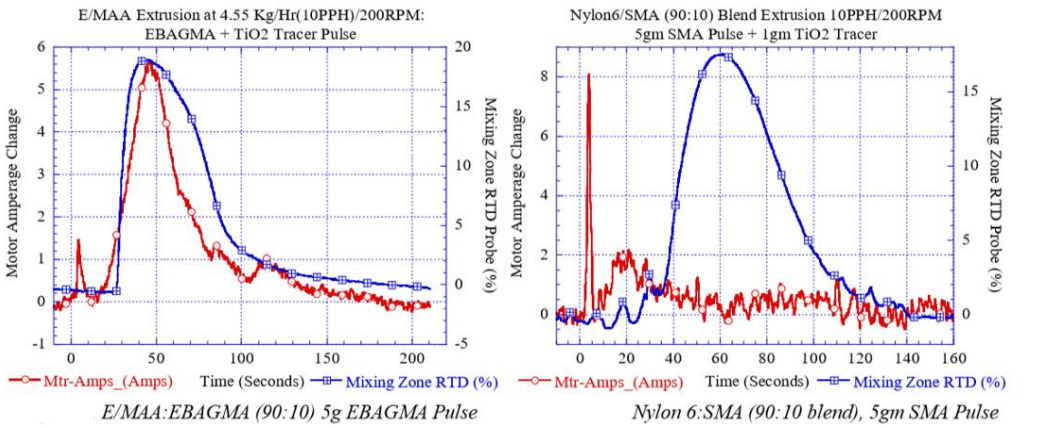


E/MAA: Ethylene/Methyl Acrylic Acid copolymer, E/BA/GMA : Ethylene/n-Butyl Acrylate/Glycidal Methacrylate terpolymer, SMA:Styrene/Maleic Anhydride

Fig.24. Analysis of the formation of polymer alloys from local residence time distribution and driving power by using "pulse-feeding" method.

### 4.2. Theoretical analysis technology for twin screw extrusion

Theoretical analysis on a twin screw extruder was first reported by A. Kaplan *et al*, targetted at a non-intermeshed counter-rotaion type twin screw extruder in 1974[25], and then was followed by J.L.

White, D.M. Kalyon, H. Potente and so on targeted at an intermeshed co-rotation twin screw extruder since 1987[26-28]. At present a lot of twin screw flow analyses used by 3D finite-element techinique have been reported and these analyses are now used for the selection of screw elements and the optimization of operation conditions for the commercial production as well as academic research[29].

**(1) Developments in 1D or 2D theoretical analysis techniques for a twin screw extruder**

Figure 25 illustrates a theoretical analysis procedure for twin screw extrusion used with a software, so-called "TEX-FAN" developed at Japan Steel Works. Using this analysis software, it is possible to estimate pressure distributions in a twin screw extruder, molten polymer temperature, melting speed and so on within short computation time, after keyed-in each geometry of screw elements and cylinder segments, operational conditions and moreover material properties. Figure 26 shows an example of these calculation results. In addition to "TEX-FAN", other similar analysis softwares are now commercialized internationally such as "Ludovic". If these softwares are used, the influence of the combination of twin screw elements or the optimization of operational conditions can be theoretically deduced with foolproof way.

Until now, empirical data were practically important to select mixing and kneading conditions for compounding inorganic filler-reinforced composites or polymer-alloys. To compare empirical data and theoretical data obtained by "TEX-FAN", Figure 27 shows some empirical data to explain a filling profile and pressure distribution at the mixing and kneading zone of a twin screw extruder for various combinations of kneading disc elements. In contrast, the use of twin screw extrusion analysis software enables to estimate quantitatively the change of pressure distributions dependent on different combinations of screw mixing elements, as shown in Figure 28.

Futhermore, twin screw extrusion analysis software "TEX-FAN" has optionally been expanded to the theoretical prediction concerning devotalization performance to remove volatile by-products, solvent and residual monomer after finished chemical reactions or polymerization[30].

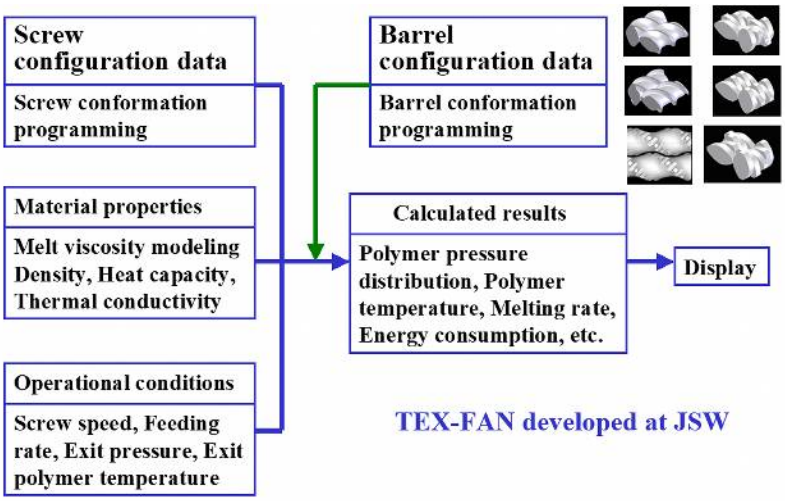


Fig.25. Computation sheme of typical extrusion characteristics for a twin screw extruder (TEX-FAN of JSW)

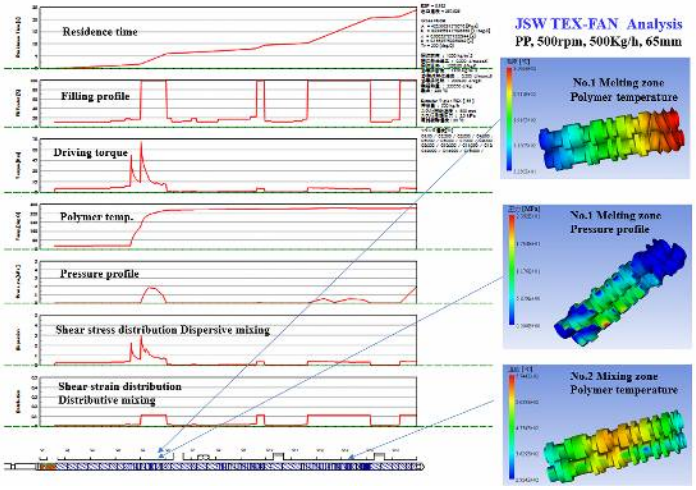


Fig. 26 Examples of simple extrusion analysis for a twin screw extruder calculated by TEX-FAN

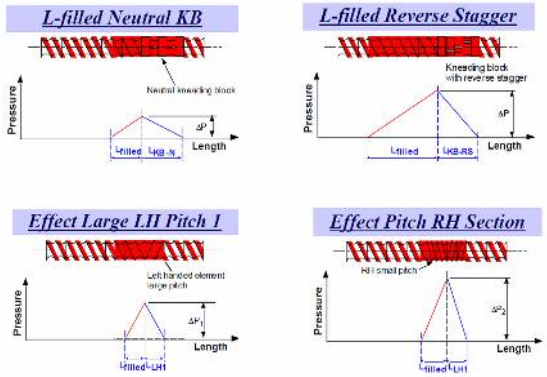


Fig.27, Relationship between kneading disc combinations and pressure profiles/filling behavior (Empirical data)

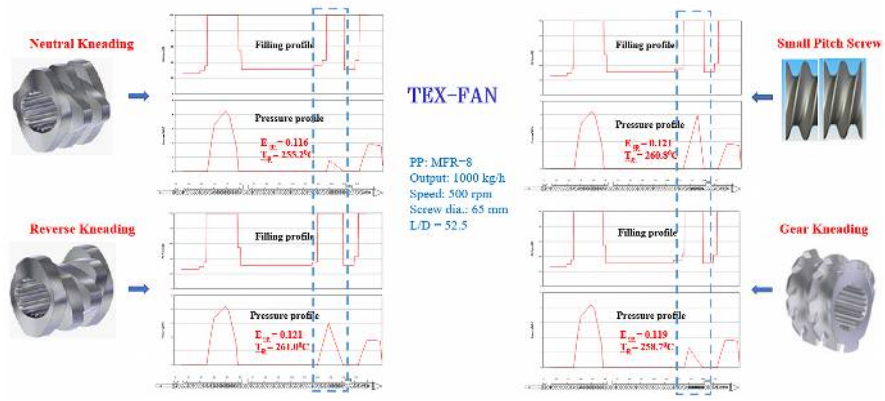


Fig. 28 Calculated examples on the relationship between kneading disc combinations and pressure profiles/ filling behavior (Theoretical data)

**(2) Developments in theoretical 3D flow analysis technology for a twin screw extruder**

Today, it is conspicuous that theoretical developments in complicated three-dimensional flow analysis technology for a twin screw extruder are rapidly progressing. Figure 29 shows one of examples on combination effects of various mixing screw elements[31]. In this study it was investigated on the difference in shear stress generation between a normal kneading disc element and a gear type mixing

element using 3D flow analysis and moreover was discussed the relationship between theoretically calculated stress distribution and glass fiber (GF) dispersion. Figure 30 shows the results on residence time distribution and shear stress distribution for each screw element under a certain operational condition. Then, Figure 31 shows the relationship between time integrated shear stress and the level of defibrilation of GF bundles. The former is obtained from theoretical computation and the latter from experimental results on defibrilation of GF bundles addded to a plastics material (polybutylene terephthalate, PBT) using a twin screw extruder. In Figure 31 it is clearly shown that closer relationship between defibrilation of GFs and minimal time integrated stress (it is equivalent to the minimal mixing and kneading energy) exists rather than that of avarage time integrated stress.

Moreover, Figure 32 shows the relationship between defibrilation ratios of GFs and the combination of each mixing screw element. The dotted line in Figure 32 shows the borderline of a permissible polymer temperature level. Judging from this line, the gear type mixing screw element of 2*D* can be applied to obtain throughput of 500 kg/h before polymer temperature reaches the upper limit (563 K). In contrast, when the kneading disc screw element is used, longer screw length can be applied before reaching the limit of molten polymer temperature (563 K) but the throughput is much lower than that of the gear type screw element. From these results shown in Figures 31-32, it is proved that higher mixing effect to make GF bundles defibrillate can be obtained with the gear type mixing screw element than that of the conventional kneading disc screw element in compounding for GF reinforced plastics. From Figure 32, it is clearly suggested that the selection of the optimum mixing screw element and productivity improvement can be achieved, if theoretical 3-D flow analysis and experimental results obtained from practical production data are combined in this way.

Complicated 3D flow analysis technology for a twin screw extruder is able to use not only for the analysis on experimental results, but also for developments in new screw design and furthermore analyses of a morphology evolution process of a polymer-alloy. Further advancement in this technology will be certainly expected in near future[32].

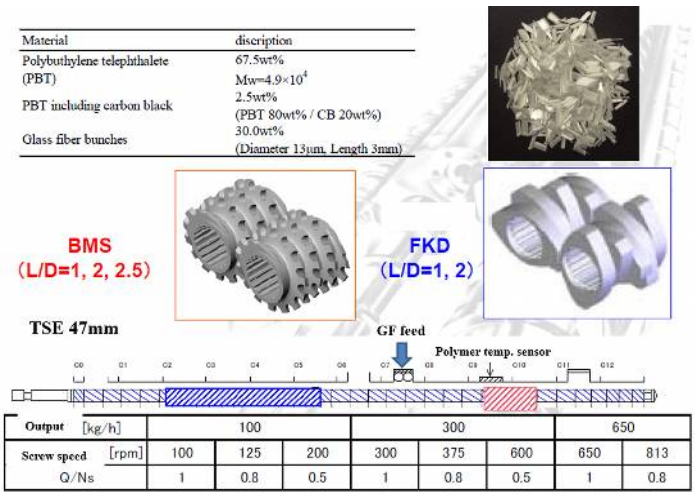


Fig.29. Experimental setup for the comparison with 3D computation results and experimental ones.

(PBT + 30% Glass fiber)

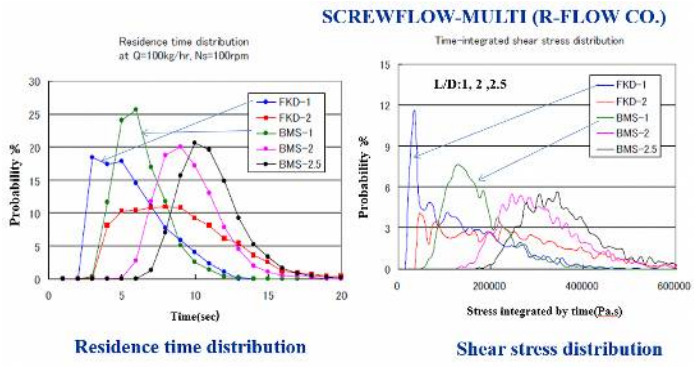


Fig. 30 Comparison of residence time distribution and shear stress distribution of conventional kneading disc elements and gear type mixing ones.

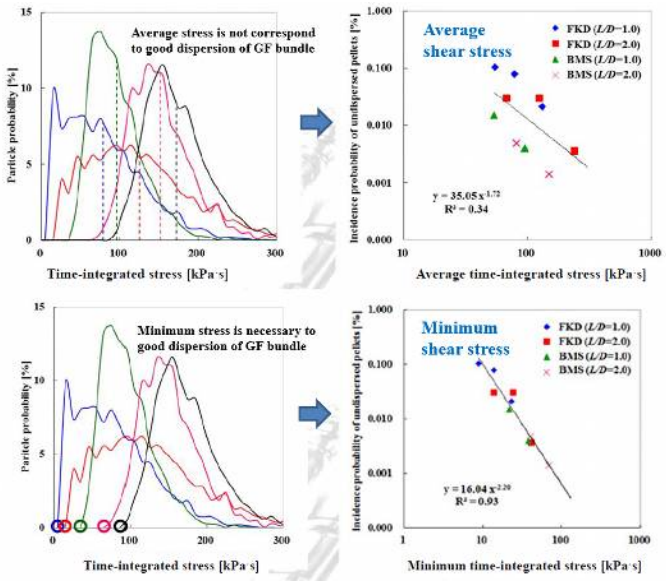


Fig. 31 Relationship between the defibliration of GFs and shear stress theoretically calculated in GF compounding.

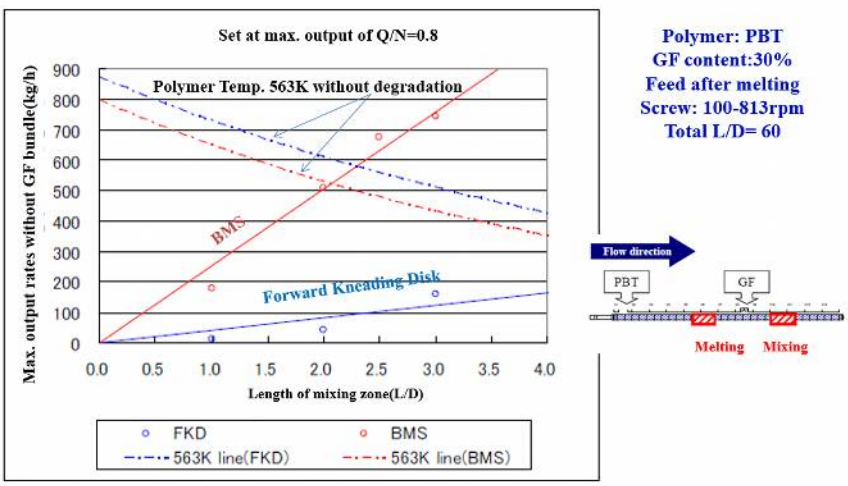


Fig.32. Comparison of kneading disc and gear type mixing element on throughput rate and quality limit in GF compounding. (FKD: kneading disc, BMS: gear type mixing element)

### 4.3. Developments in new techniques for the selection of various twin screw element combination

#### (1) Searching for optimum twin screw combination by using genetic algorithm optimization

To achieve further progress in the polymer processing industry, the evolution for digitalization technology in the manufacturing fields is indispensable[2]. Today, technology establishment such as production line monitoring, theoretical analysis and process modeling of various polymer processing methods are essential as one of key factors to lead toward futher advancement.

An attempt to seek the optimum solution for screw element selection was applied to a twin screw extruder using genetic algorithm optimization[33]. Genetic algorithm is a technique that realizes the solution on a lot of optimization problems, adapting a basic genetic mechanism of nature for computation. Figure 33 shows an evolutional procedure of multi-objective optimizaion algorithm to fix the optimum screw design for a twin screw extruder[33]. In this study three set of screw elements were selected at random with combinations of four kneading discs, left-handed (backward) screw elements and right-handed (forward) screw elements in the melting zone and mixing/kneading zone of a twin screw extruder of $L/D$ = 24. Extrusion characteristics at each zone were analyzed using twin screw analysis software "Ludovic". In the first stage the best combination of screw elements was separately assigned to fit with each target value, such as residence time, shear strain, polymer temperature and energy consumption. Figure 34 shows the best screw element assembly (No.1-No.5) selected under suitable operating conditions (the constant screw speed and throughput rate) respectively in accordance with this procedure shown in Figure 33. Then, the final screw element combination was optimized to satisfy all of the targets using multi-objective evolution algorithm by trial and error, and the result was shown in the bottom (No. 6) of Figure 34.

The search precision can be gradually improved after the plural answers (the optimum solution to achieve extrusion targets related to product's properties) on screw design are obtained, if applied with multi-objective evolution algorithm.

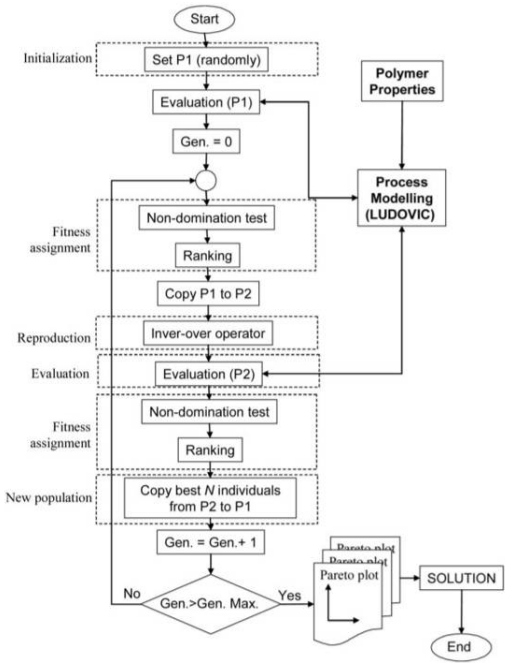


Fig. 33. Multi-objective evolution algorithm scheme for the best screw element selection.

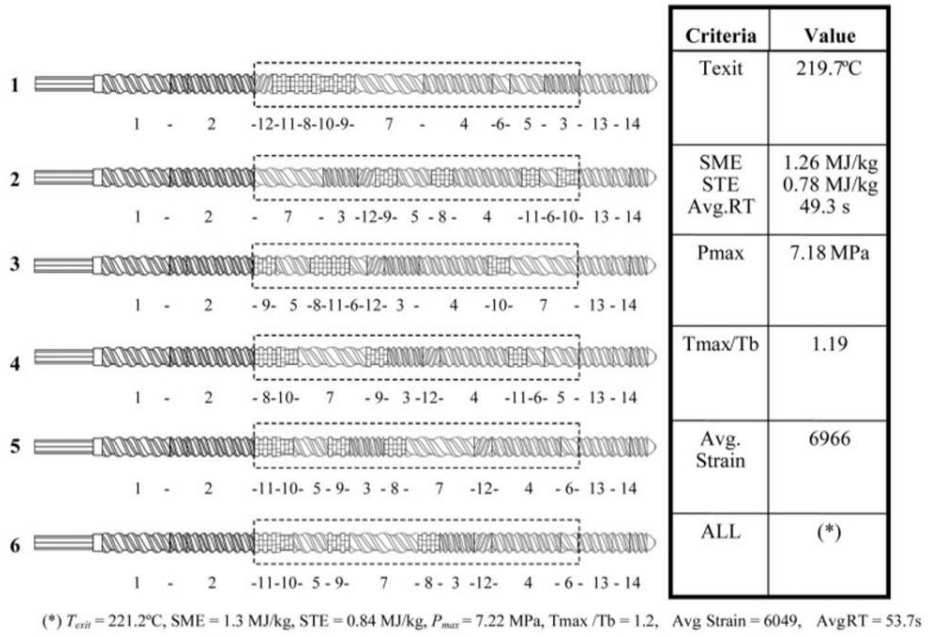


Fig. 34. The results on selected screw element combinations to fit with target values using multi-objective evolution algorithm (Throughput $Q$ =10 kg/h, Speed $N$=200 rev/min and $T_b$ =200 $^0$C)

**(2) Searching for optimum twin screw combination by using AI technology**

In this section progress of AI (Artificial Intelligence) technology in the plastic compounding field was discussed.

The following is an example that a combination of theoretical computation technology and AI technology was used for the selection of various twin screw elements in compounding[34]. First, several kneading disc canditates were randomly selected for the melting zone ($L/D$= 4) of a twin screw extruder and then a series of experiments to evalulate melting behavior under constant operational conditions were carried out. At the same time melting analysis for each pre-set screw combination was taken place using twin screw extrusion analysis software "TEX-FAN"[30]. Figure 35 shows the experimental results and theoretical calculation ones (as teacher data). Next, the combination of the screw elements that would be achieved complete melting under constant operational conditions was output from the teacher data using Deep Learning of AI.

Figure 36 shows Deep Learning procedure of AI and computation output on some screw element combinations deduced by AI technology. When the screw element combinations derived from AI technology were compared with the ones based on conventional knowledge from past experience, the clear difference appeared. An examle is that less number of right-handed (forward) screw elements was selected by AI technology, although we usulally use a certain number of right-handed screw elements for compounding operations. Furthermore, Table 1 is the experimental results to prove the applicability of the screw element combinations derived from AI technology. From Figure 36 it is obvious that the screw element assembly derived from AI technology showed good agreement with the final targets such as designed polymer temperature and melting behavior.

Screw design to use compounding operations is one of the most important factors that deeply affect product quality and productivity, but the factor is conventionally determined from experience by trial and error due to the complexity connected with various factors. As shown the case introduced here, the feature of this AI technology utilization is not only the extraction from accumulated past data, but also to deliver the optimum solution based on knowledge obtained from the enormous quantity of the past experiments. Therefore, the recognition accuracy can be increased and perfection degree of the computation solution can be inevitably improved, if a system accumulates successful examples as much as possible. In other words, the level of the achievment is determined whether the amount of data accumulated in the past is large or not.

In near future it is surely expected that the utilization of AI technology will be greatly advanced in various polymer processing fields, including in the compounding field.

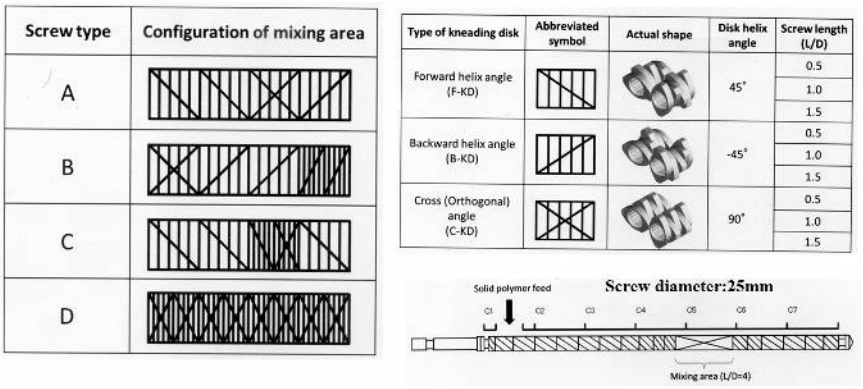


Fig. 35. Preliminary experiments for various kneading disc design (for teacher data acquisition)

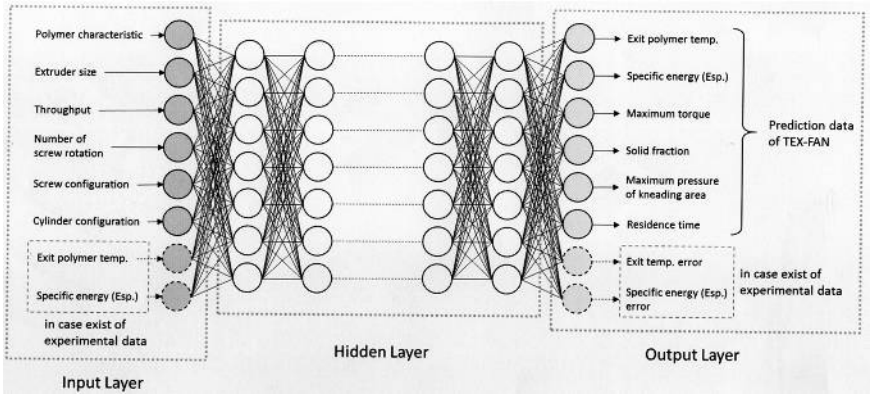


Fig. 36. Procedure for Deep Learning on twin screw design

Table 1. Experimental verification for TEX-FAN analysis and AI prediction

| | Screw type | Determination of machine learning | conformity | Prediction of FAN analyze | Experiment |
|---|---|---|---|---|---|
| E | E | 200.0[℃] | 99.6% | 209.7[℃] | 201.0[℃] |
| F | F | 200.0[℃] | 99.3% | 212.0[℃] | 200.0[℃] |
| G | G | 200.0[℃] | 99.1% | 211.3[℃] | 199.7[℃] |
| H | H | 200.0[℃] | 99.0% | 211.5[℃] | 198.7[℃] |

## 5. Developments in compounding technology used with a twin screw extruder

### 5.1. Compounding technology focused on nano-clay

A nano-size filler is more remarkable in specific surface area and cohesion force between each filler particle, when compared with a conventional inorganic filler. In such a system, it is suggested that each particle is not dispersed easily, even if large shear stress is loaded for mixing. Therefore, single use of mechanical mixing and kneading actions is generally impossible to make each particle disperse discretely and then the utilization of physico-chemical reaction to raise the miscibility is indispensable, when mixing and kneading of molecular scale is requested.

B.Vergnes published excellent review on several melt-blending methods for the nanocomposite compounding focused on nano-clay dispersion[35].

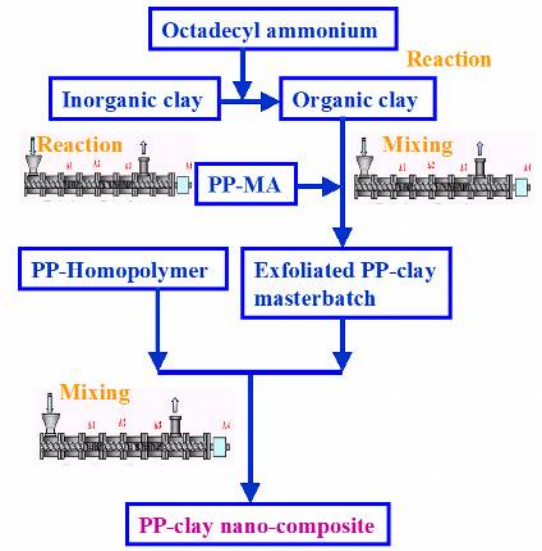


Fig. 37 Conventional nanocomposite production process (master batch method)

Figure 37 shows a typical process to produce a polymer nanocomposite by melt-blending. Because of the difficultiy in dispersion of nano-clay in a polymer matrix, affinity improvement on the surface of nano-clay should be treated as so-called “organification”. Then, a graft-copolymer bonded with polar-group such as maleic anhydride is needed to be added as a compatibilizer to increase compatibility between nano-clay and the polymer matrix.

From Figure 38 to Figure 40 some research results are shown on the influence of screw rotational speed, throughput and moreover shear stress in melt-blending so as to disperse nano-clay in polypropylene (PP) matrix homogeneously[35-37]. These results show that better nano-clay dispersion was obtainable under higher shear stress, higher screw speed and lower throughput in compounding.

In contrast, other researchers reported that distributive mixing (total shearing strain) dominates the nano-clay dispersion in melt-blending. Judging from these experimental results, it seems that the theoretical mechanism in nano-clay dispersion has not been well established yet[38].

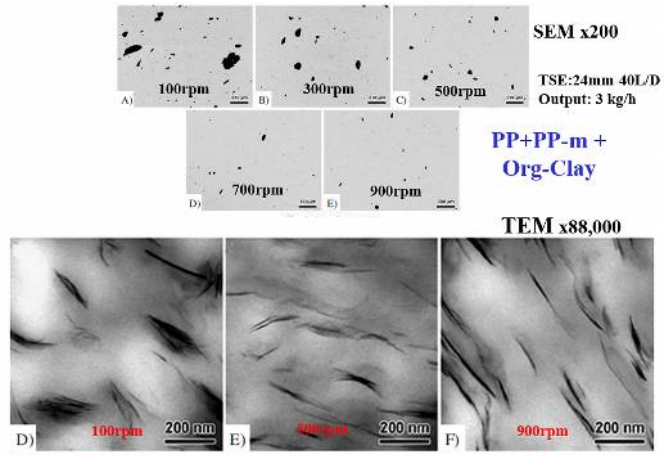


Fig. 38 Influence of screw rotational speed on dispersion of nano-clay

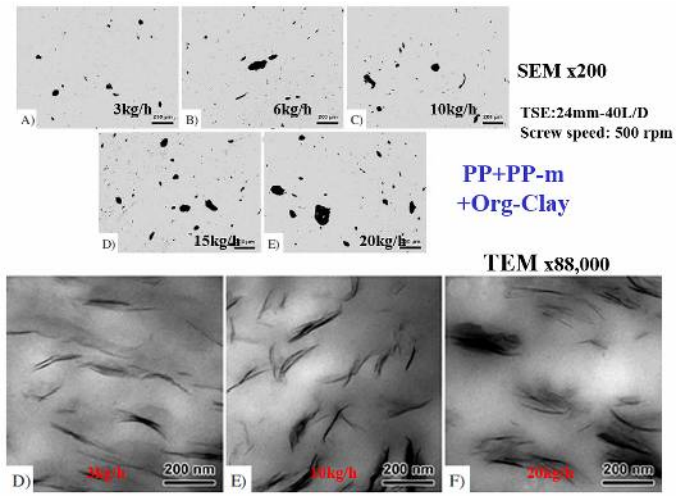


Fig.39. Influence of throughput on dispersion of nano-clay

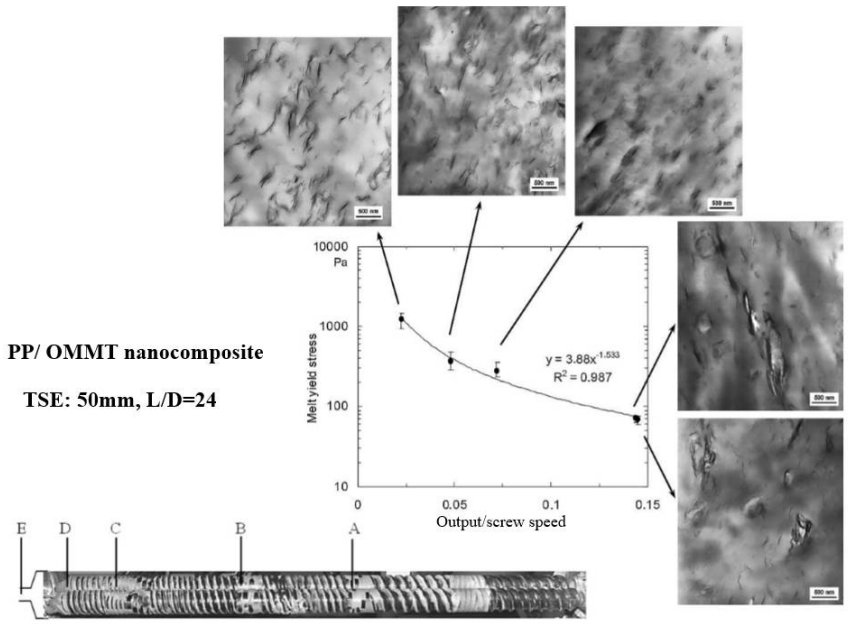


Fig. 40. Relationship between of shear stress and nano-clay (OMMT) dispersion

To obtain polymer blends with nano level morphology and further to produce polymer nanocomposites with excellent physical properties, chemical affinity around phase boundaries is eccential. Recently, an epoch-making melt-blending method for nano-clay compounding was developed by injecting a large amount of water to a molten polymer directly into a twin screw extruder[39-41]. Figure 41 shows a practical example that a high-performance nanocomposite was developed by adding large amount of water directly to amorphous polyester. It is reported that the nanocomposite obtained from this process exhibited high product quality, although no organizing treatment on the nano clay surface was applied only with water addition. It is because the exfoliation of nano-clay platelets is easily occurred in aquaous solution (water slurry) and a polymer temperature falls down by heat removal owing to steam evaporation from a twin screw extruder and furthermore melt-viscosity elevation (this means shear stress increase for mixing). As a result, dispersive mixing actions are much accelerated.

The other research to be introduced is the use of supercritical fluid as a dispersion accelating medium. When supercritical fluid is injected in a molten polymer, both the reduction in melt-viscosity and the change in the boundary surface tension between the polymer matrix and nano-clay are observed at the same time , and hence better dispersion of nano-clay is obtainable. The research and development to use this effect are continuously progressing[42].

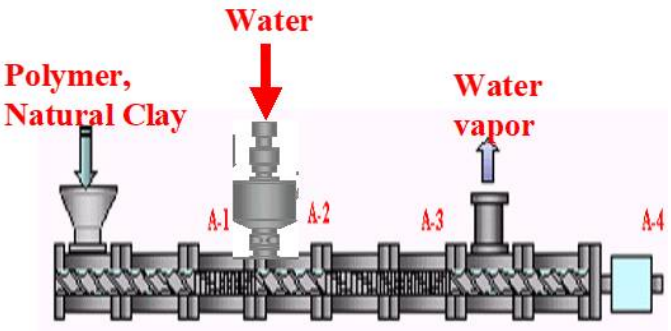


Fig.41. Manufacturing processes of amorphous polyester nanocomposites used by water assisting

### 5.2. Compounding technology on carbon nano-tube (CNT)

#### (1) Conventional compounding method for CNT

H. Takase *et al* reported that the dispersion of CNT in the polycarbonate (PC) matrix could be experimentally evaluated by total shear strain (product of shear rate and residence time) in compounding using a twin screw extruder, but in contrast the fracture of CNT was increased vigorously under high shear strain, which provoked considerable deterioration of electric conductivity of PC/CNT composites, as shown in Figure42[43,44]. In conclusion, they found the optimum operational conditions so as to lead excellent electric conductivity, compromising with CNT length reduction.

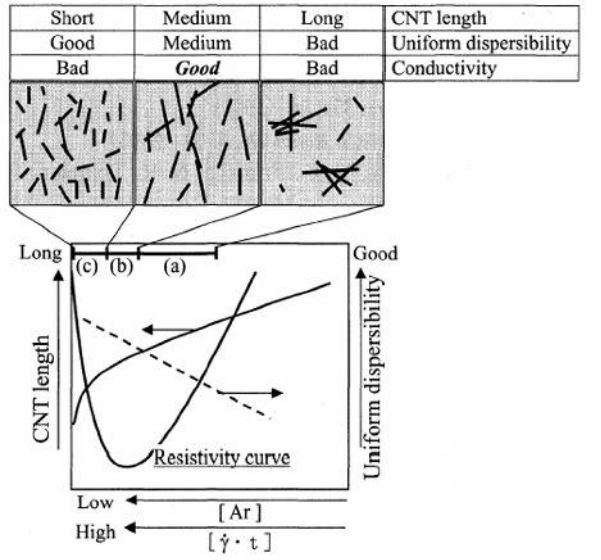


Fig.42. Relationship between compounding conditions and electro-conductive performance of PC-CNT (3%) composites

Today, multi-wall CNT (MWCNT) has been widely used. However, single-wall CNT (SWCNT) is now drawn much attention because of its excellent potentialities. The problem is that the dispersion of SWCNT into a polymer matrix is much more difficult when that of MWCNT is compared. Figure 43 shows the influence of operational conditions and screw design of a twin screw extruder on the dispersion of SWCNT in a PP matrix. To obtain better dispersion of SWCNT, screw design focused on high dispersive mixing or operations under high screw speed posessed positive tendency to improve[45]. That is to say, it is suggested that dispersive mixing actions (shear stress) played an important role in promotion of the SWCNT dispersion as shown in Figure 43.

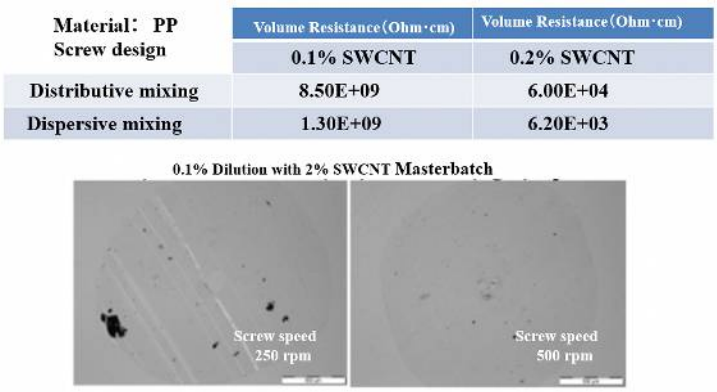


Fig. 43. Influence of screw design and operational conditions on CNT dispersion and volume resistivity of PP/SWCNT composites

### (2) Compounding of CNT by utilizing elongational mixing

Researches aimed at improvement in CNT dispersion have been reported lately using special twin screw elements with high elongational mixing capability[46,47]. It is because dispersive mixing effect is better than that of shear mixing, if elongational mixing is applied in melt-blending.

Figure 44 shows the difference in CNT dispersion between conventional kneading disc screw elements and specific screw elements (EME) with elongational mixing capability. This result shows that the screw elements with elongational mixing capability performed better dispersion of CNT[46].

Moreover, Figure 45 shows evaluated results on mixing and kneading effects of this screw element with elongational mixing capability for immiscible polymer blends (PP/PS)[47]. Even if melt-viscosity difference between two polymers is large, the decrease of the domain size was more remarkable when elongational mixing screw elements (EME) were used. In shear flow mixing, it is generally difficult to obtain high mixing effects in polymer blending with large viscosity ratios. However, from Figure 45 it was verified that the use of elongational mixing is greatly effective in compounding for polymer blends with large viscosity ratios.

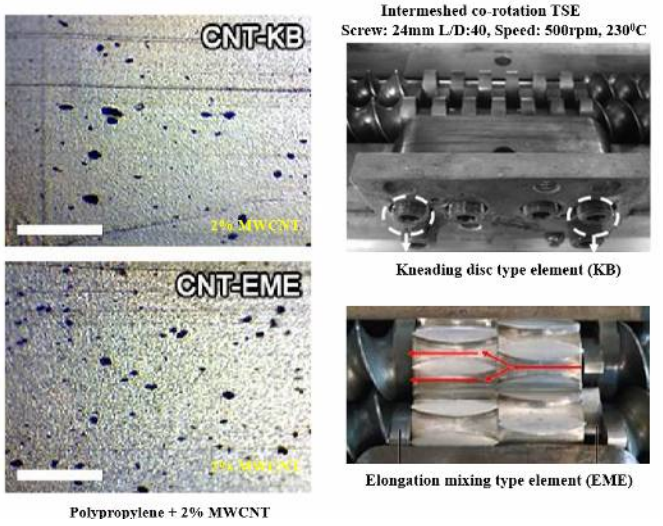


Fig. 44. Effects of different mixing screw elements on dispersion of MWCNT

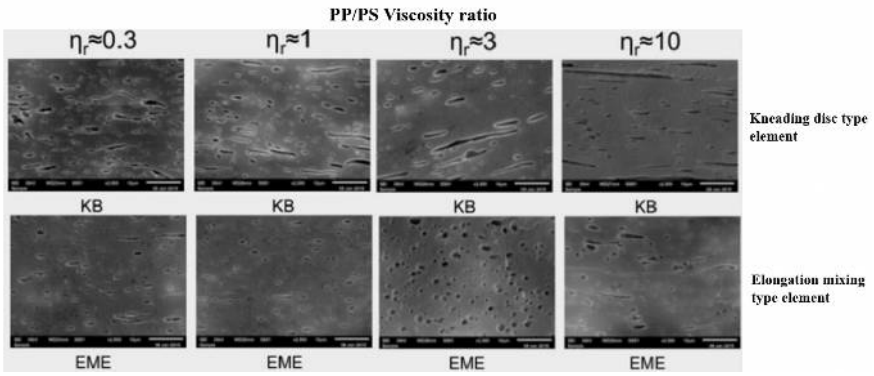


Fig.45. Effects of different mixing screw elelments on morphology of PP/PS polymer blends with various viscosity ratios

Moreover, K. Matsumoto investigated comparison of dispersion degree of CNT between a conventional mixing screw element and an elongational mixing screw element used for compounding with a twin screw extruder[48]. In his research, he carried out experiments used with various screw elements to evaluate elongational mixing effects. Figure 46 shows combinations of various mixing screw elements inserted at the mixing and kneading zone of a twin screw extruder. Furthermore, Figure 47 shows the

relationship between the aggregate size of CNT, the geometry of mixing screw elements and operational conditions, and suggests that the aggregate size was declined in order of conventional kneading disc type, gear type and elongational mixing type. From these results it is cleary suggested the use of elongational mixing is effective in dispersing MWCNT as a difficult-to-mix material.

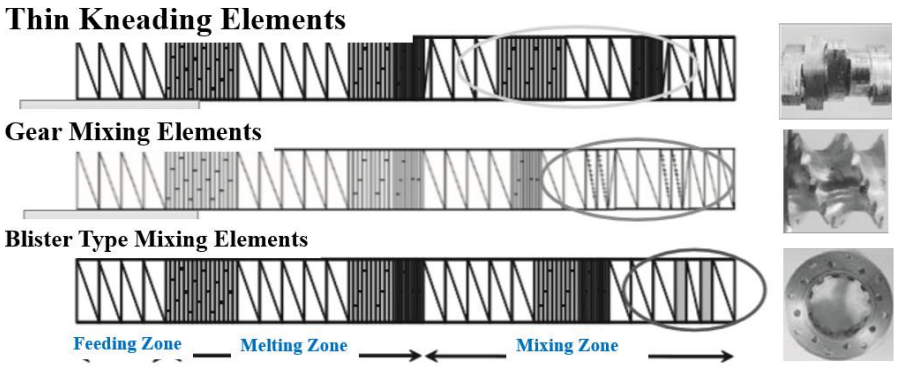


Fig.46. Various mixing screw elements to evaluate MWCNT dispersion

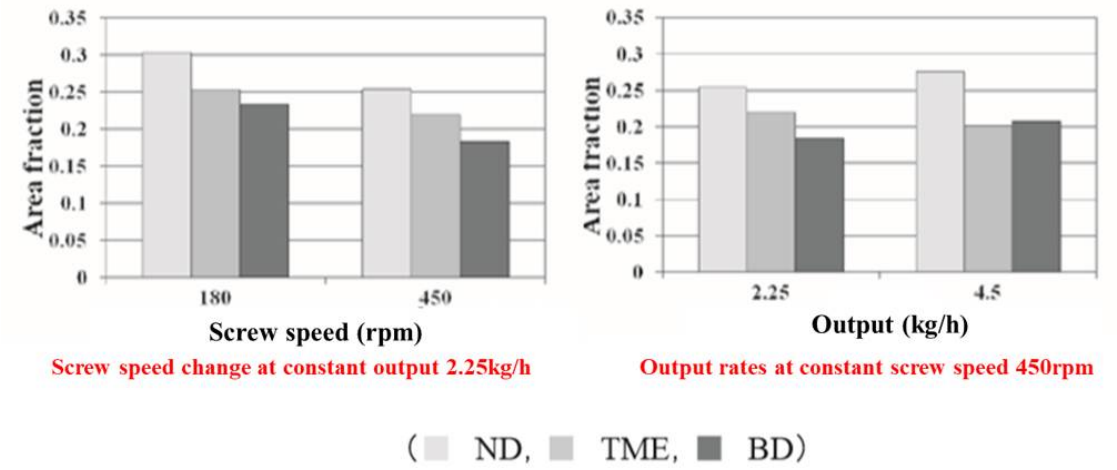


Fig.47. Influence of various mixing screw elements on MWCNT dispersion

**(3) Compoounding of CNT by utilizing a water-assist (water-slurry)method**

In the previous section it was reported that better nano-clay dispersion was attained when nano-clay was suspended in water in advance. Similar to this process, the use of a water-slurry process (water-assist compounding) is very effective to promote CNT dispersion in melt-blending. In this research CNT is suspended in advance with a suitable deflocculating agent and is fed into a twin screw extruder. Figure 48 shows the outline of the difference in dispersion degree of CNT between a conventional melt-blending method and a water-assist one[49], and suggests that the water-assist method can induce higher dispersion degree of CNT. Moreover, Figure 49 shows that electric conductivity of various comounds obtained from different compounding methods. This Figure clearly shows that better conductive characteristics were obtainable even with smaller addition of CNT, when the water-assist method was used in melt-blending.

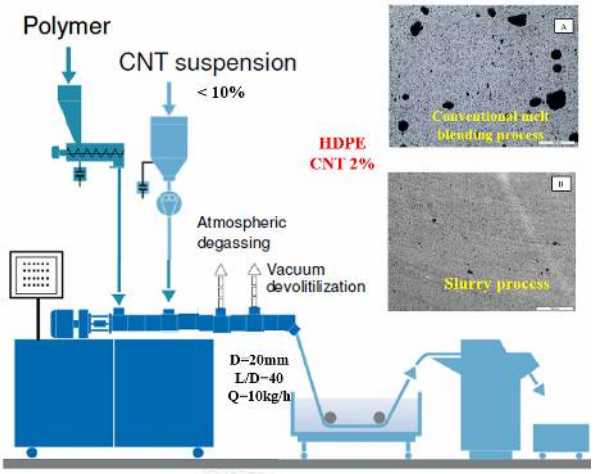


Fig.48 Compounding system of nanocomposites used by a water-assist method

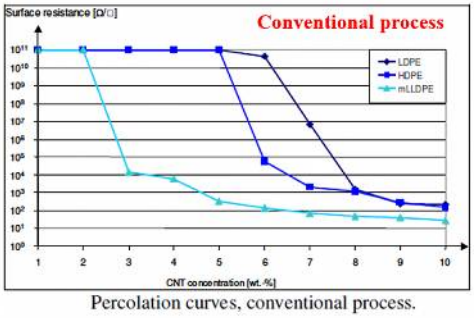


Percolation curves, conventional process.

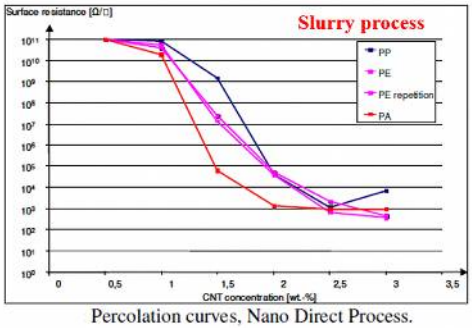


Percolation curves, Nano Direct Process.

Figure 49. Difference in CNT percolation characteristics obtained by different compounding process

#### 4) Compounding of CNT applied by polymer blending techniques

CNT is a high-priced material and therefore is requested to reduce amount of the addition as low as possible. One of the ways to reduce the addition of CNT is the utilization of morphology control of a polymer-alloy after preblending CNT with a polymer which is easy to disperse in advance.

Figure 50 shows graphically-demonstrated aspect of nano-clay transition between two kinds of polymers during compounding operations. As shown in Figure 50, in a mixing process nano-clay gradually migrates to rubber phase having higher compatibility after nano-clay is first mixed together with rubber of lower compatibility (A), and then new morphology (D) is formed after a certain time of mixing[50,51].

Figure 51 is an practical example how to obtain higher electric conductivity of polystyrene (PS) by the addition of CNT. In this case, localized dispersion of CNT is induced by the addition of polymer blends

composed of polyvinylidene fluoride (PVDF)/high-density polyethylene (HDPE)[52]. In general, CNT is easy to disperse in the PS phase, but larger amount of CNT addition is necessary when required higher electric conductivity only by blending with PS and CNT. However, if PVDF is incrementally added, the relative concentration of CNT is increased in the PS phase because CNT does not migrate to the PVDF phase. As a result, the electric conductivity of PS/PVDF blends is considerably improved. Moreover, when HDPE with no compatibility with PS/PVDF polyblends is subsequently added, the electric conductivity obtained is drastically improved because the PS phase with CNT is only localized around the boundary layer of PVDF and is formed an efficient conduction path as shown in Figure 51.

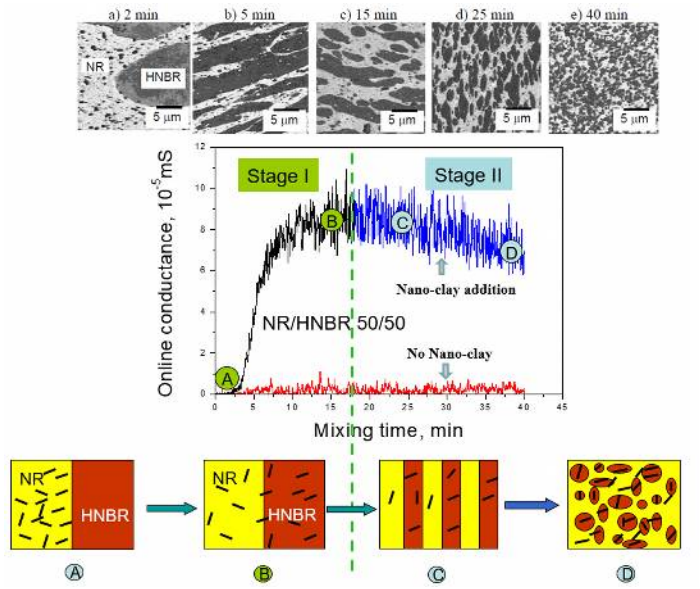


Fig.50. Filler transfer behavior in compounding for a nano-clay composite

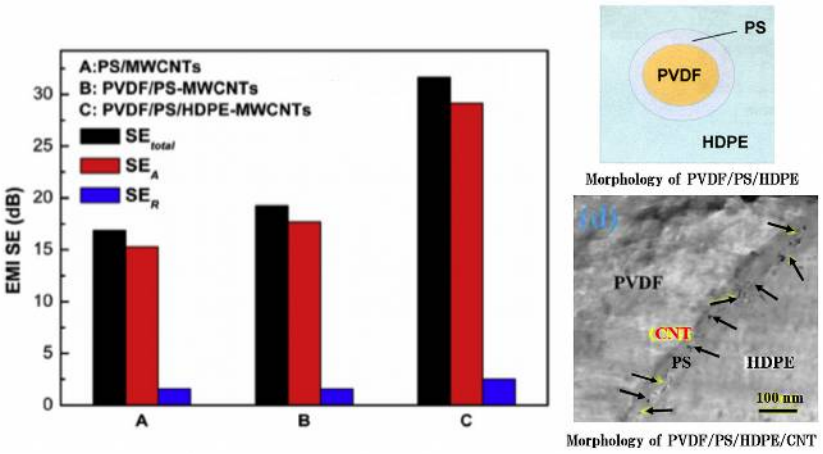


Fig.51. The relationship between the improvement of EMI characteristics and the morphology formation related to various MWCNT composites

As other sophisticated example, K.Fukumori *et al* reported a new technique that can control both thermal conductivity and electrical insulating properties of CNT reinforced polymer-blends at the same time by using complicated morphology manupulation of a polymer-alloy[53]. It is general that high

mechanical strength and thermal conductivity are obtainable but electrical insulating properties are declined when CNT is added. However, a product with high electrical insulating properties, keeping with high thermal conductivity, is sometimes requested in the specified market. Figure 52 is one of examples that such contradicting requirements was achieved by controlling polymer-alloy morphology composed of Nylon 6 (PA 6) and polyphenylenesulfide (PPS) [53]. The following is a procedure how to obtain polymer blends with high thermal conductivity, keeping with high electrical insulating properties. First, the PPS domain of nano-size was formed in the PA matrix contained with CNT by melt-blending. Second, PA/PPS/CNT blends with high thermal conductivity and high mechanical strength were produced by using GOPTS (Glycidylpropyl-trimethoxy-silane), *i.e.* a shell structure forming agent to encapsulate each edge of CNT, while electrical insulating properties were maintained. Furthermore, Figure 53 shows the comparisons of electrical insulation properties and thermal conductivity of various PA/PPS/CNT blends obtained through several compounding prescriptions. In case of the blend shown as "F" in Figure 53, high thermal conductivity and high mechanical properties were simultaneously achieved, while high electrical insulating property was maintained.

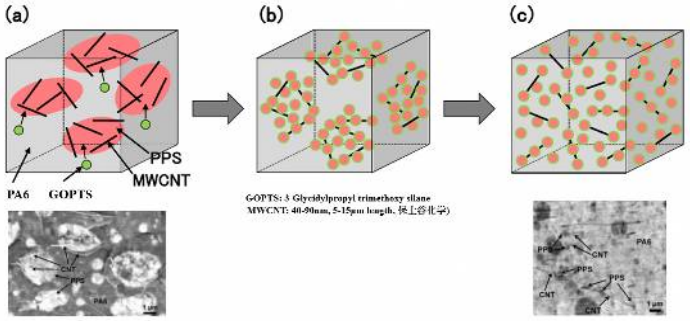


Fig.52. A new compounding process to control both thermal conductivity and volume resistivity by sophisticated PA/PPS/CNT alloy-blending

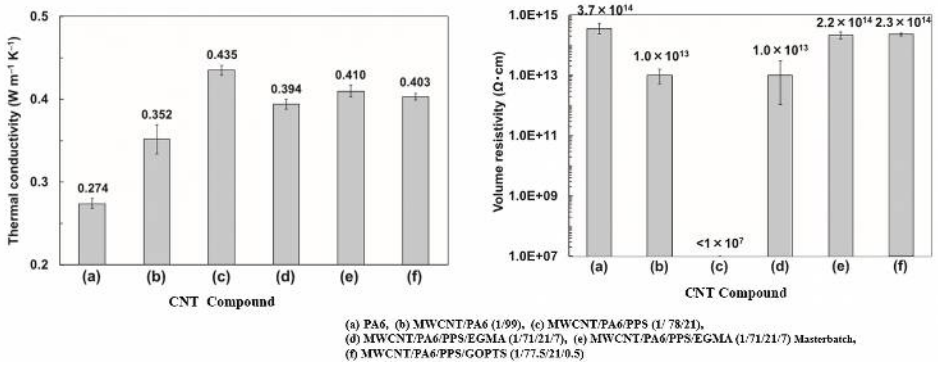


Fig.53. Thermal conductivity and volume resistivity of PA/PPS/CNT compounds through various mixing processes

## 6. Developments in polymer-alloy creation technology using twin screw compounding.

In creating polymer-alloys using with a twin screw extruder, melt-viscosity ratio, compatibility and surface tension (capillary number) play an important role. Furthermore, to promote chemical reactions, mixing and kneading efficiency, polymer temperature and moreover residence time (and its distribution)

in the extruder are very important[4]. Therefore, new techniques how to combine these factors are essential for creating highly functional polymer-alloys.

In this section recent developments in compounding technology using a twin screw extruder are introduced.

### 6.1. Compounding for polymer-alloys with complicated phase-morphology of nano-scale

Not only the creation of polymer composites filled with nano-size inorganic additives is becoming popular, but the creation of polymer-alloys with nano-level morphology is also progressed along with technical advancement in a twin screw extruder having higher mixing capability[54-56]. Figure 54 shows the difference between conventional polymer-alloys and new ones with nano-level morphology. Such fine morphology is only possible to be formed by the optimization of a mixing and kneading process using a twin screw extruder and the selection of proper compatibilizers to fit with a target blending system. Furthermore, Figure 55 shows the relationship between mechanical properties of two kinds of PC/ABS polymer-alloy and thickness of injection-molded products[56]. In typical PC/ABS polymer-alloy, impact strength was dropped significantly as increasing product thickness. However, PC/ABS polymer-alloy with nano-level morphology possessed relatively stable impact strength, even though the thickness of injection-molded products considerably varied.

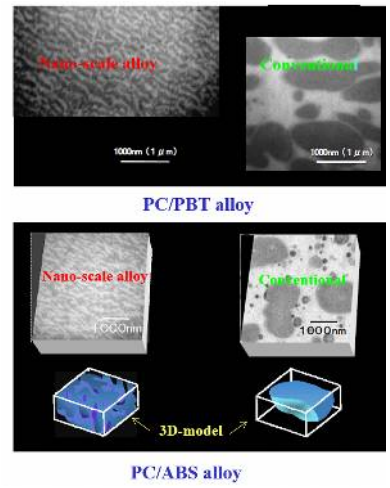


Fig. 54. Comparison of morphology between conventional polymer-alloys and nano-scale ones

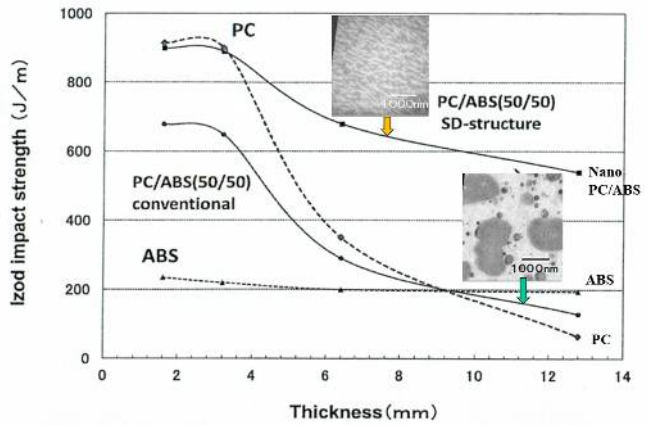


Fig. 55. Difference in impact strength of PC/ABS alloys with different morphology

Moreover, Figure 56 shows an example to attempt improvement in mechanical properties of a polymer-alloy by nano-scale morphology formation[57]. In this case, the morphology of a polymer-alloy composed of bio-base polyamide 11 (PA11) and PP was precisely controlled to obtain higher mechanical strength. In the first stage, PA11/PP polymer-alloy with salami structure was produced to obtain higher mechanical strength. In the next stage, PA11/PP polymer-alloy with co-continuous morphology was produced to perform the highest mechanical strength. Two kinds of PA11/PP polymer-alloys exhibited higher mechanical properties, when compared with PA11/PP polymer-alloy having sea-island structure that was created using conventional compounding technology. The difference of each morphology is shown in Figure 56. The scale of salami structure is also attained to nano-level as shown in this Figure.

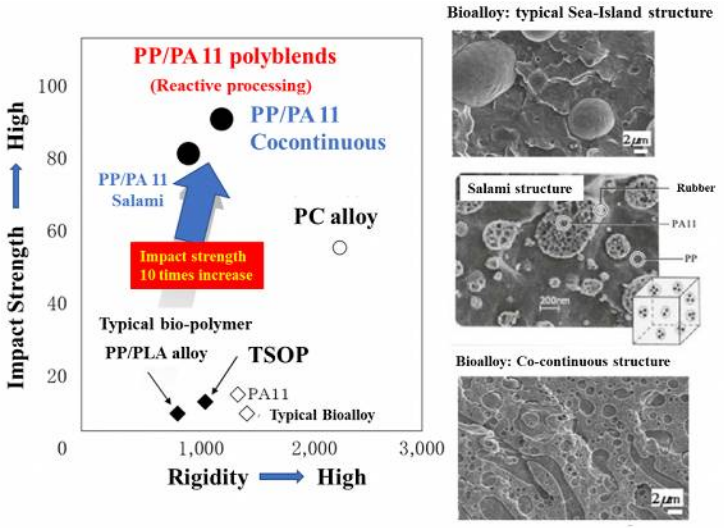


Fig.56. Improvements in impact strength of PP/PA-11 alloys produced by morphology control.

### 6.2. Compounding used a dynamic vulcanization process.

#### (1) Comparison between dynamic vulcanization and simple polymer blending

Figure 57 shows the relationship between material characteristics and morphology of two kinds of polymer blending, that is, dynamic vulcanization and simple polymer blending[50, 51]. The big difference in morphology of polymer-alloys is clearly shown between compounding procedures accompanied with cross-linking reaction and without cross-linkage reaction using a twin screw extruder.

The formation of the morphology is deeply influenced with characteristics of polymer alloys, e.g., molecular-structure, melt-viscosity, melt-elasticity, and surface-tension. It is also deeply affected with operational conditions of a twin screw extruder, such as polymer temperature, pressure profile, shear rate, residence time, feeding location and so on.

In a dynamic vulcanization system, rapid viscosity elevation of a rubber phase triggered by cross-linking reaction brings about phase inversion in a polymer alloy. Important factors to cause phase inversion and domain size fixation are cross-linkage reaction speed and mixing conditions.

Figure 58 shows a process for morphology formation of a polymer-alloy in a twin screw extruder. This was obtained by a screw pulling-out method to visualize morphology changes during dynamic vulcanization operations. Different from pure mechanical blending, the morphology changes after

feeding a vulcanizing agent are clearly shown, that is, phase-inversion and domain size minimization caused by dynamic vulcanization.

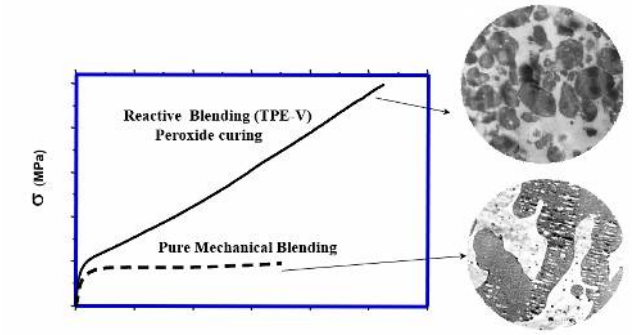


Fig.57. Comparison of mechanical properties and morphology of each polymer-alloy obtained by a simple blending process and dynamic vulcanization one, respectively.

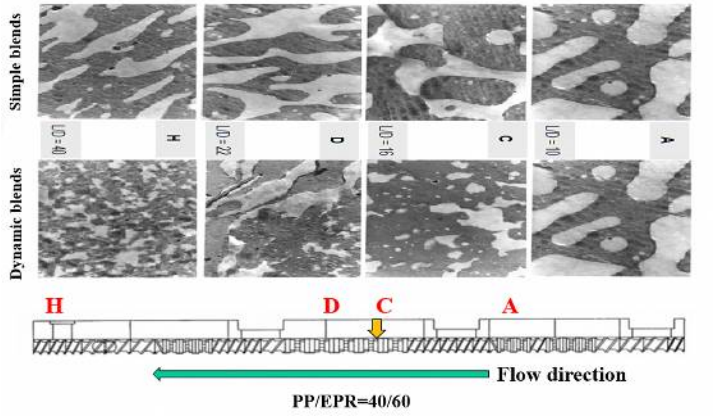


Fig.58. Difference in morphology formation between a dynamic vulcanization process and a simple blending one

**(2) New polymer-alloy creation technology by using a dynamic vulcanization process**

For long time polyvinyl chloride (PVC) has been widely used for wire coating, but lately it was rapidly converted into polyolefin from the viewpoint of solid-waste management.

Figure 59 and Table 2 introduce an example that a new wire coating material was developed by using compounding technology[58]. In this project a dynamic vulcanization process was used to obtain a substituting material instead of PVC. The substituting material was applied to ethylene-vinyl acetate copolymer (EVA) and scheme of a dynamic vulcanization process is shown in Figure 59.

In the first step a graft-copolymer of EVA was generated in amorphous EVA by mixing and kneading using a twin screw extruder after fed with a silane coupling agent. In the next step the compound was mixed with crystalline EVA and then with a fire retardant in sequence. In this stage the domain phase is crystalline EVA (thermoplastic polymer), and the matrix is amorphous grafted-EVA (rubber). Moreover, cross-linking reaction in amorphous EVA was continuously performed by feeding a cross-linking agent into a twin screw extruder. Accordingly, amorphous EVA was changed from the matrix phase to the domain by phase-inversion. Meanwhile, the crystalline EVA was converted into the matrix during dynamic vulcanization due to rapid melt-viscosity increase of amorphous EVA by

cross-linking reaction. As a result, the compound obtained from this process changed thermoplastic elastomer, which is applicable to normal extrusion processing. The product properties are totally equal to those of conventional PVC for wire coating as shown in Table 2.

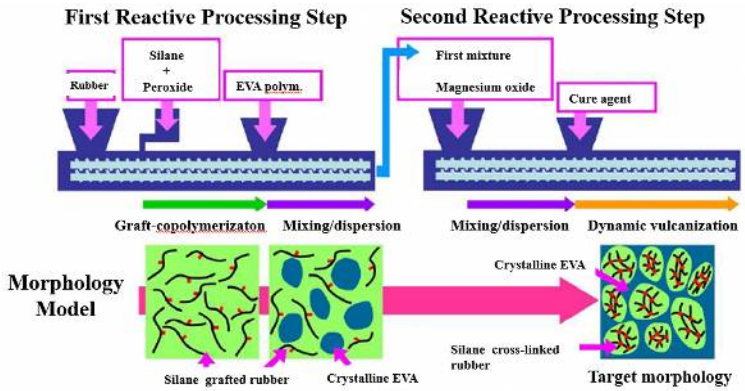


Figure 59. Development of a new wire coating material by reactive processing

(Hitachi Cable Co.)

Table 2. The properties of newly-developed wire-coating material produced from EVA by dynamic vulcanization (comparison with conventional coating material, PVC)

| Item | Specification | Target | New product | PVC product |
|---|---|---|---|---|
| Tensile | Tensile strength (MPa)<br>Elongation (%) | ≧ 10<br>≧350 | 12.9<br>390 | 19.3<br>350 |
| Heating 90°C, 96 h | Remained tensile-strength(%)<br>Remained elongation (%) | ≧ 80<br>≧ 65 | 120<br>95 | 101<br>100 |
| Oil resist. 70°C, 4h | Remained tensile strength(%)<br>Remained elongation (%) | ≧ 60<br>≧ 60 | 78<br>80 | 98<br>90 |
| Heat deform. 75°C, 15N | Thickness reduction (%) | ≦ 10 | 8.7 | 7.9 |
| Low temp. resistance | -15°C | No crack | No crack | No crack |
| Flame retardation | | 60 seconds | Passed | Passed |
| Flexibility | 10% modulus (Mpa) | ≦ 2 | 0.8 | 0.8 |

### (3) Recycling of waste rubber using a dynamic vulcanization process

K. Fukumori *et al* reported an innovative manufacturing process for thermoplastic-elastomer starting from waste rubber used for car parts[59]. In this process cross-linkages of waste vulcanized rubber are selectively broken down by shear stress generated in a twin screw extruder with high-rotational screw speed and the waste rubber was regenerated to vulcanizable rubber again. Then dynamic vulcanization is applied to the regenerated rubber after added polypropylene (PP) as a thermoplastic polymer matrix.

Figure 60 shows this process to regenerate from waste ethylene-propylene rubber (EPDM) to vulcanizable rubber by cutting cross-linkages under a high shearing operation using a twin screw extruder. By injecting a certain amount of water into the twin screw extruder and then vaporizing as steam through a venting port, both large heat removal and extraction of bad-odor ingredients generated

by thermal degradation of rubber were skillfully taken place. Simultaneously, higher shear stress necessary for cross-linkage scission was additionally increased in this process by water injection. Figure 61 shows a scission mechanism of the cross-linkage bonds by high shear stress. It is well-known that bonding force of the cross-linkage of EPDM is lower than that of main polymer chain, and therefore it is considered that shearing force can attack selectively on this cross-linkage bonding because of lower activation energy.

Moreover, Figure 62 shows a dynamic vulcanization process with the addition of a PP component using a twin screw extruder to converts continuously into thermoplastic-elastomer. This is a process to convert waste rubber into thermoplastic-elastomer, which is applicable to general a polymer processing method such as extrusion or injection molding. In the initial stage, waste EPDM was converted to vulcanizable EPDM at the first mixing zone of a twin screw extruder and then a dynamic vulcanization operation was taken place at the second mixing zone. It was reported that the thermoplastic elastomer product obtained from this process is reusable for some parts of a car again.

On the other hand, C. Tzoganakis *et al* developed a different technique to regenerate a waste tire efficiently by injecting supercritical CO2 fluid into a twin screw extruder. The future progress is worth noting[60].

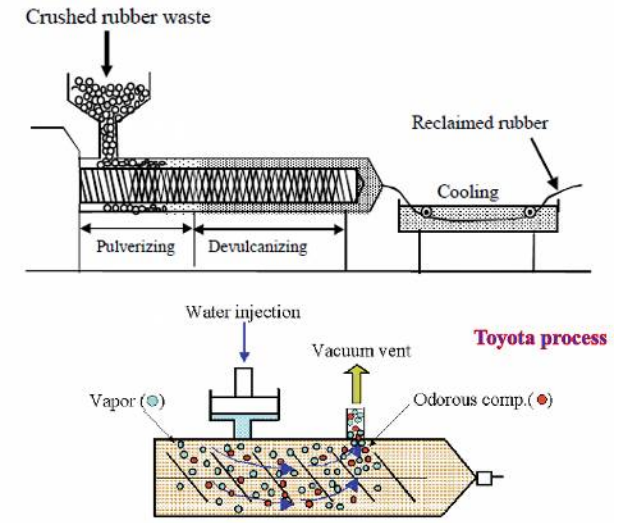


Fig. 60. Waste EDPM reclaiming process used with a twin screw extruder.

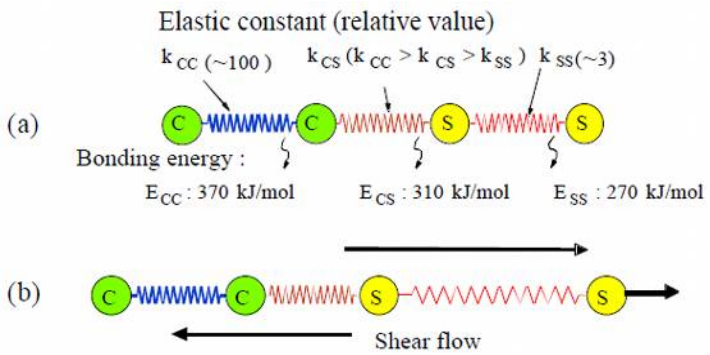


Fig. 61. Fracture mechanism on breaking-up cross-linkages of waste rubber under high shear stress

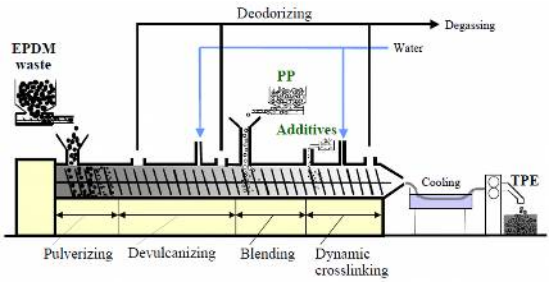


Fig.62. Continuous process to produce thermoplastic elastomer from waste EPDM.

### 6.3. Compounding of dynamically vulcanized rubber with a fire retardant

It is practically important to mix a fire-retardant to dynamically-vulcanized rubber used for lots of industrial applications. However, mechanical strength of a compound easily declines if added high amount of a fire retardant. N. Lopattananon *et al* reported good results in obtaining compounds with less mechanical property deterioration but with improved flame retardancy by optimizing compounding procedures[61-63].

Figure 63 shows two kinds of mixing procedures, *i.e.*, conventional mixing and master-batch mixing for compounding high amount of a fire retardant, aluminum hydroxide (ATH), and vulcanizing agents to natural rubber (NR). Furthermore, Figure 64 shows each dispersion state of a fire retardant after compounded by these mixing and kneading procedures. From this Figure it is clearly observed that the fire retardant was only dispersed in the NR phase of the compound obtained from the conventional mixing procedure. In contrast, the fire retardant was dispersed both in the NR phase and in the PP phase of the compound obtained from the master-batch mixing procedure.

Moreover, Table 3 shows the evaluation results of the combustion characteristics of each compound by cone-calorimetry and limiting-oxygen-index (LOI). The compounds obtained from the master-batch mixing procedure (SMB) possessed better combustion performance with the minimum addition of the fire retardant. And in addition, the decline of mechanical strength was suppressed when compared that from the conventional mixing procedure (CV). In this study it was further reported the dispersion state of ATH in the PP phase caused deep influences on combustion characteristics, judging from GC-MASS analysis to evaluate flammable decomposed substances in combustion[63].

Figure 65 shows a manufacturing process how to deal with this compounding operation continuously using a twin screw extruder. If combining different twin screw extruders tandemly, the mixing and kneading actions both for a fire retardant and for dynamic vulcanization can be efficiently and continuously performed[64].

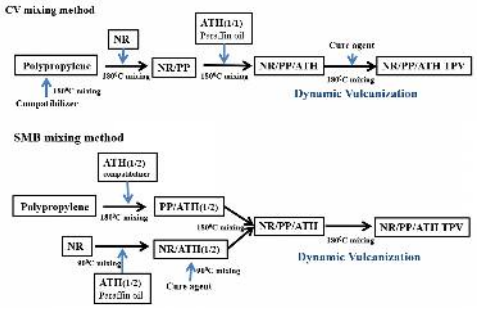


Fig. 63. Compounding procedure of a fire retardant (ATH) for dynamically vulcanized NR/PP

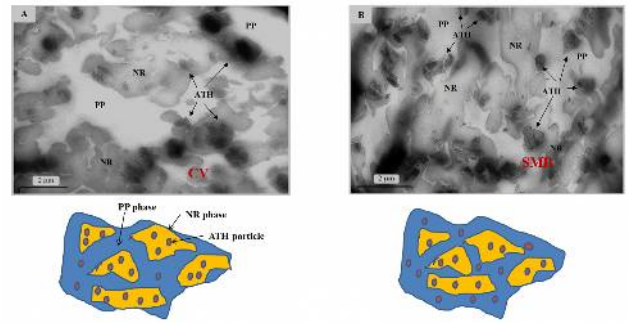


Fig.64. Difference in fire retardant distribution of NR/PP dynamic vulcanizates between CV and SMB.

Table 3. Comparison of flame resistance of NR/PP vulcanizates obtained by different mixing procedures.

| Sample | LOI ↓ | TTI (s) | PHRR ($kW/m^2$) | THR ($MJ/m^2$) | Ave. HRR ($kW/m^2$) |
|---|---|---|---|---|---|
| Neat CV- TPV | 16.7 | 15.1 | 721.6 | 184 | 454 |
| CV-TPV-ATH60 | 21.7 | 19.9 | 440.4 | 91 | 333 |
| SMB-TPV-ATH60 | 24.2 | 22.4 | 420.5 | 92 | 318 |
| CV-TPV-ATH80 | 25.0 | 22.2 | 381.2 | 72 | 279 |

LOI: Limiting Oxygen Index, TTI: Time-To-Ignition, PHRR: Peak Heat Release Rate, THR: Total Heat Release Rate

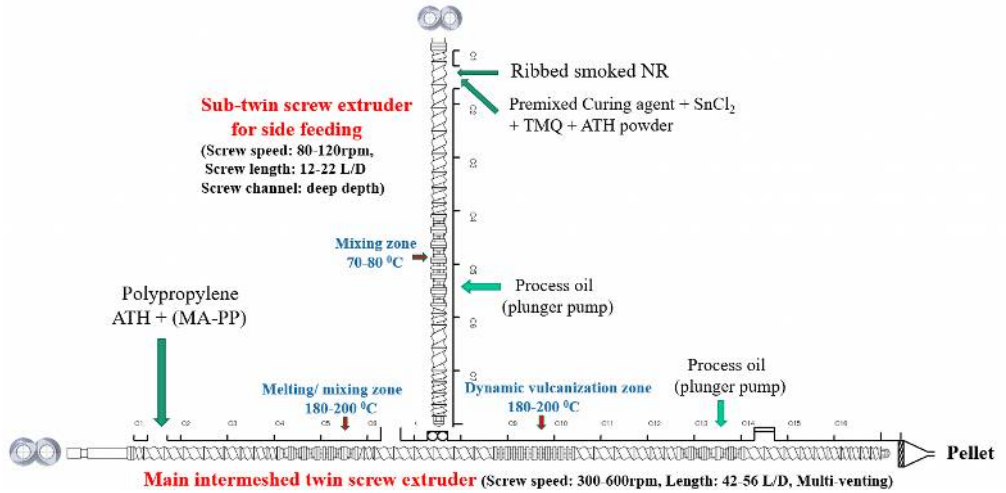


Fig. 65. Continuous compounding process of NR/PP vulcanizates with a fire-retardant using twin screw extruders tandemly.

### 6.4. Morphology control of natural rubber composites by utilizing nano-clay addition.

S. Ray *et al* reported that the morphology of PS/PP(50/50) polymer-alloys is conspicuously changed, when nano-clay is added during polymer blending operations just like compatibilizer addition[65]. Furthermore, T. Sakai *et al* confirmed the domain size reduction of a polymer-alloy, when adding

nano-clay in polymer blends based on NR[66]. In this study they proved compatibilizing effects of nano-clay by 3-D micro-X-ray tomography analysis and TEM observation. For example, Figure 66 shows the observation results on compatibilizing effects of small amount of nano-clay in a blending system of NR/PP. It was observed that the size of a rubber phase was reduced and the boundary-layer around a PP phase was changed ambiguous as increasing nano-clay concentration. That is to say, the addition of nano-clay brought about both reinforcing effects and also compatibilizing effects, when nano-clay was added into the blending system of NR/PP.

On the other hand, NR is a natural biopolymer collected as latex form from rubber trees. It is usually commercialized after coagulating/dewatering processing. As shown in Figure 67, NR/PP/nano-clay composite can provide considerably higher degree of mechanical properties than those of conventional NR/nano-clay ones or simple NR/PP binary polymer blends. To produce the composite, a nano-filler or nano-fiber was first mixed to NR latex and subsequently polypropylene (PP) was added under strong mixing and kneading conditions after de-watering(drying) NR/nano-clay slurry[66]. Figure 68 shows the morphology comparison of two kinds of NR composites. From this Figure it is suggested that a kind of synergetic reinforcement mechanism in the NR/PP/nano-clay composite was brought about by compatibilization effects of the nano-clay addition and fiber-reinforcement effects of the PP component induced by strong shearing force in a twin screw extruder.

Furthermore, Figure 69 explains a fiberizing mechanism of the PP component by shearing force in a twin screw extruder. In the first step, NR mixed with nano-clay in NR latex in advance was mixed with the PP component at a high temperature above melting point ($T_m$) of PP. In this stage, the PP component was dispersed in the NR/nano-clay component by strong mixing and kneading. In the next step, a vulcanizing agent was added to the NR/PP/nanoclay composite below $T_m$ of PP and further mixing was continued. The PP component in the NR/PP/nanoclay composite was intensively drawn by shearing force and was changed to the fibril-form without remelting, if the mixing temperature was controlled above glass transition($T_g$) temperature of PP and below $T_m$ of PP. In the last step, the NR/PP/nano-clay composite was hot-pressed and vulcanized at high temperature such as 180$^0$C to obtain a cured product. The fibrillated PP component still maintained with fibril-form even after the vulcanization treatment owing to the retaining force of nano-clay platelets localized around the boundary of the PP fibrils. In contrast, the PP component in the NR/PP composite without nano-clay did not maintain the fibril-form because the fibrillated PP was naturally changed to particle-form due to remelting under high vulcanization temperature. As a result, the PP particulates contributed to lower reinforcement effect than the PP fibrils.

Based on the total process described here, T.Sakai *et al* proposed a new production process to manufacture continuously a unique NR composite with high-mechanical properties utilizing a twin screw extruder[64]. Figure 70 shows an innovative production process. This process is an extremely complicated system that combined various sophisticated compounding techniques such as slurry-mixing, de-watering, compatibilizing and self-fiberizing. To apply this continuous compounding system, nano-clay is mixed sufficiently with NR latex using a high-speed mixer prior to producing NR/PP/nanoclay composite in the first. In the next step this mixture is supplied to the twin screw extruder together with a coagulating agent. In this step the NR/nano-clay component is coagulated from large amount of water

and is separated from water by squeezing and vaporizing operations using a special cylinder furnished with a lot of slit. After the de-watering treatment on the NR/nano-clay component, a PP component is fed continuously into the dried NR/nano-clay component and is well mixed using the twin screw extruder at high temperature above $T_m$ of PP. In the last step a vulcanizing agent is added to the NR/PP/nano-clay compound and moreover is mixed at proper polymer temperature between $T_g$ and $T_m$ of PP. In this last step the pre-vulcanized NR/PP/nano-clay composite reinforced with the fibrillated PP component is obtained continuously. This composite having high-mechanical properties will be applicable to various industrial rubber products in the market.

Highly advanced technologies for compounding using a twin screw extruder are strongly expected for developments in creating highly functional polymer-alloys and related nano-composites in near future as demonstrated in this review.

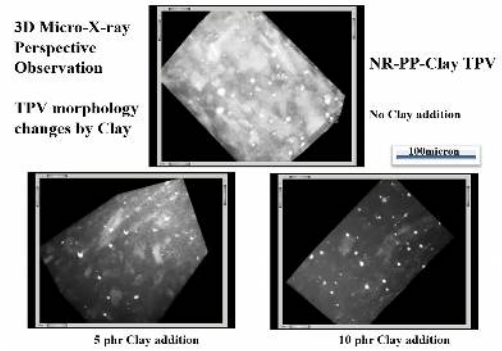


Fig. 66. Change in morphology of NR/PP dynamic vulcanizates by nano-clay addition.

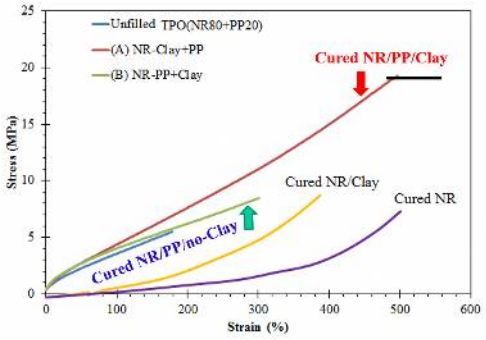


Fig. 67. Mechanical properties of NR composites reinforced by fibrillated PP component.

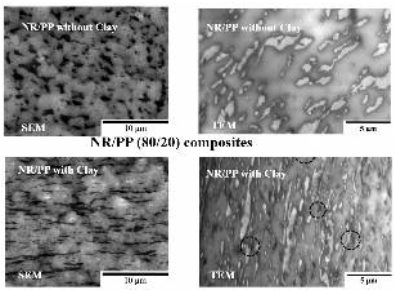


Fig. 68. Difference in morphology of NR/PP composites with nano-clay and without nano-clay

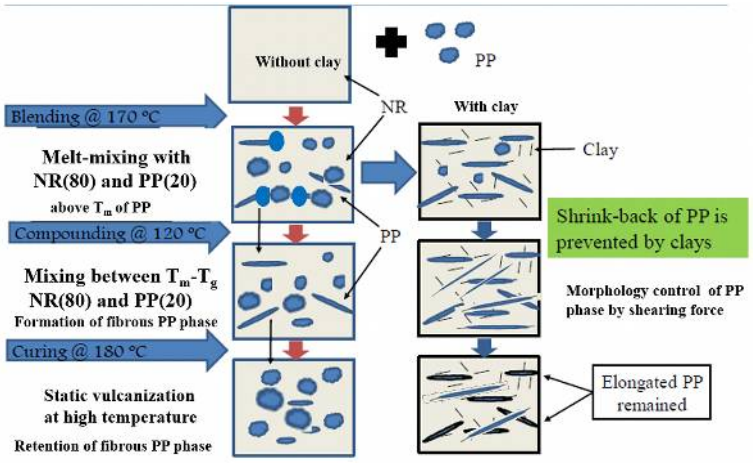


Fig. 69. Self-reinforcement mechanism of NR/PP/nano-clay composites with fibrillated PP component

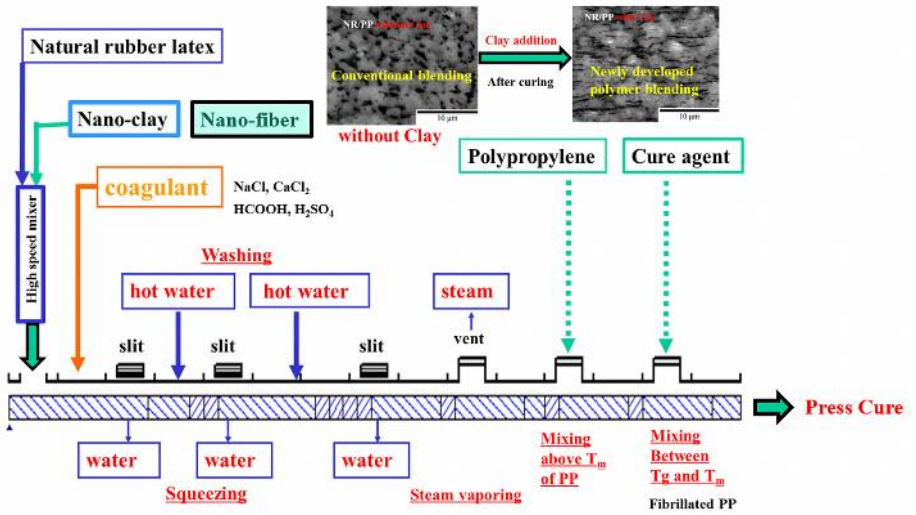


Fig. 70. Continuous compounding process for manufacturing newly-developed NR/PP/nano-clay composites using with a twin screw extruder.

## 7. New mixing and kneading techniques and mixing equipment.

### 7.1 New technique concerning kneading disc design.

It is conventionally general that the shape of each screw element is symmetrically designed for an intermeshed co-rotation twin screw extruder. On the other hand, special development in asymmetrical kneading disc design was reported to attempt the improvement in mixing and kneading effects[67]. Figure 71 shows the comparison with a conventional kneading disc with symmetrical geometry and newly developed one with asymmetrical geometry. A self-cleaning effect is rightly maintained for both screw design. Moreover, Table 4 shows flame retardancy and mechanical strength of ABS compounds with a typical flame retardant of aluminum phosphate obtained with two kinds of kneading discs. The compound obtained by using with an asymmetrical kneading disc was achieved high fire-resistance as well as excellent mechanical properties.

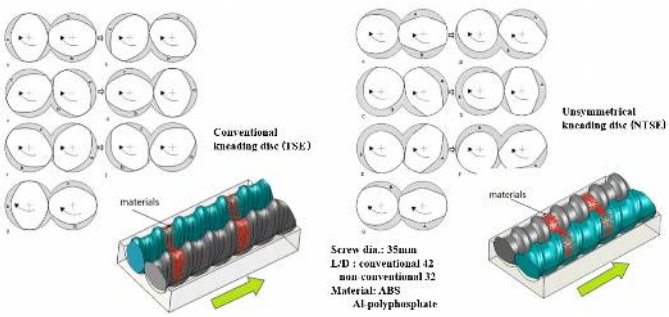


Fig. 71. Rotational motion compared with conventional kneading discs and asymmetry kneading discs

Table 4. Comparison of mechanical properties and flame retardancy of ABS/Phosphate compounds obtained by the conventional kneading discs and the asymmetrical ones

Mechanic properties of ABS/IFR composites from TSE and NTSE

| Extruders | TSE | NTSE |
|---|---|---|
| Notched impact strength/ KJ/m$^2$ | 5.44 | 6.89 |
| Tensile strength/ MPa | 10.11 | 12.76 |
| Elongation at break/% | 16.40 | 26.36 |

Flame retardant properties of ABS/IFR composites from TSE and NTSE

| Extruders | TSE | NTSE |
|---|---|---|
| LOI | 24.1 | 26.2 |
| UL-94 Rating | V-0 | V-0 |
| Dripping | No | No |
| AFI | 0/9 | 0/6 |

**AFI** is average flaming time after the first or the second ignition.

### 7.2. Vane type extruder

A vane type extruder is attracted attention as a new extruder having no screw rotation mechanism. Figure 72 shows the structure of this extruder. The vane type extruder can work as a compounding and/or molding device just like a conventional single screw extruder or twin screw one. Furthermore, it was reported that the mixing and kneading capability of a vane type extruder surpasses a twin screw extruder, because compulsory elongational mixing actions can be generated along with the rotational movement of the vane[68-70]. As a result, more compact design of a vane type extruder is applicable and the compounds with higher dispersion are obtainable when a conventional single screw extruder is compared.

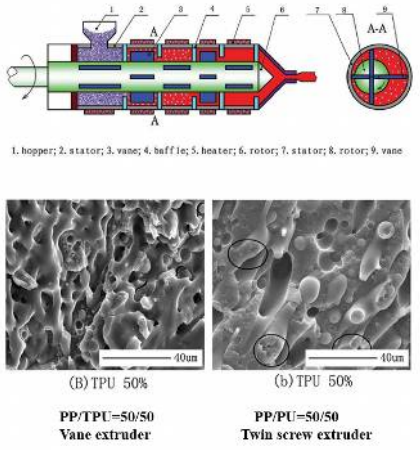


Fig. 72 The structure of a vane type extruder and the comparison of each morphology of PP/PU alloys obtained from a vane type extruder and conventional twin screw one.

### 7.3. Ring type multi-screw extruder

A ring type extruder is a kind of an extruder that has the structure installed several sub-screws around one principal screw axis. Various mixing screw elements can be set up along the sub-screws as same as an intermeshed co-rotational twin extruder. Figure 73 shows the structure of a ring type extruder. It was reported that this extruder possesses high compounding capabilities such as distributive mixing, elongational mixing and excellent devolatilization[71,72]. Such new extruder that can perform higher mixing and kneading characteristics different from a conventional twin screw extruder is strongly required and is attracted attention from the point of special applications to new engineering polymer composites with advanced functionality.

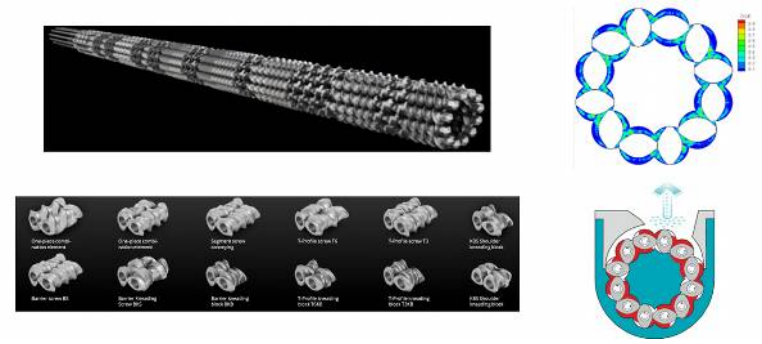

Fig.73 Structure of a ring type extruder and a screw element system

## Concluding remark

In addition to remarkable developments in system design technology on a twin screw extruder, lots of new compounding techniques used with a twin screw extruder have been rapidly spreading in these days. Long years have been already passed after the establishment of basic concept on a twin screw extruder around 1930's. Maintaining this basic concept on the extruder structure, innovative developments have been carried out, for examples, various screw elements with highly efficient mixing/kneading capability, high screw driving power with large torque density and moreover sophisticated theoretical analysis techniques for twin screw compounding. As a result, a lot of technology have been applied to create very wide variety of polymer-alloys and polymer nano-composites with highly-additional-values using a twin screw extruder for compounding.

In this article, recent technical advancements in twin screw compounding were widely reviewed. The author hopes that this review can give some suggestions on future research and development in creating highly functional polymer alloys and related composites.

## Literature


1) T.Sakai, *Plastics Age*, **61** (6), p46 (2015)
2) T.Sakai, *Plastics Age*, **65** (1), p45 (2019)
3) T Sakai, *Plastics Age*, **64** (6), p40 (2018)
4) T.Sakai, *Plastics Age*, **58** (6), p56 (2012)
5) P.Anderson, *Plast. Eng., April.* p32 (2013)
6) T.Sakai, *Plastics Age*, **55** (6), p52 (2009)

7) M.Wetzel, C-K.Shih, D.Deneslbeck, S.Latimer, SPE ANTEC 2005, ( 2005)
8) V.Collin, *et al* , *Appl. Polym. Sci,* **2,** p121 (2013)
9) A.Y.Malkin, A.V.Baranov, *et al*, *Int. Polym. Proc.,* **8 (**2), p99 (1993)
10) H.P.Grace, *Chem. Eng. Commun.,* **14,** p225 (1982)
11) J.E.Loukus, A.C.Halone, M.Gupta, SPE-ANTEC 2004, p133 ( 2004)
12) M.Bouquey, C.Loux, B.Triki, R.Muller, PPS-24 Annual Meeting, Salerno , ( 2008)
13) M.Tokihisa, K.Yakemoto, T.Sakai, L.A.Utracki, M.Sepehr, J.Li, Y.Simard, *Polym. Eng.& Sci.,* **40,** p1040 (2006)
14) T.Kajiwara, H.Tomiyama, A.Uotani, S.Inoue, K.Funatsu, *Seikei-Kakou*, **18 (**11), p819 (2006)
15) Seikei-Kakou Symposia (Toyama), p49 (2014)
16) Y.Zhang, C.Tzoganakis, SPE-ANTEC 2005, p394 ( 2005)
17) B.Luo, Z.Long, S.Sun, SPE-ANTEC 2007, p382 ( 2007)
18) X.Ma, S.Ren, Q.Liu, Y.Yin, X.Geng, SPE-ANTEC 2005, p372 ( 2005)
19) G.Fukuda, D.Bigio, B.Dryer, *et al*, SPE ANTEC 2015 (2015)
20) S.Tenge, D.Mewes, *Polym. Eng. & Sci.,* **40** (2), p277 (2000)
21) T.Sakai, *Adv. Polym. Techn.,* **14** (4), p277 (1995)
22) T.Sakai, *Plastics Age*, **59** (6), p66 (2013)
23) M.Wetzel, D.Denelsbeck, C.K.Shih, SPE-ANTEC 2003, p3791, ( 2003)
24) C-K.Shih, [Mixing and Compounding of Polymers, Chapter 15] Hanser (2009)
25) A.Kaplan, Z.Tadmor, *Polym. Eng. & Sci.,* **14,** p58 (1974)
26) W.Syzydlowski, J.L.White, *Adv. Polym. Techn.,* **7,** p177 (1987)
27) D.M.Kalyon, A.D.Gotsis, C.G.Gogos , C.Tsenoglou, SPE-ANTEC 1988, **34**, p64 ( 1988)
28) H.Potente, J.Ansahl , R.Wittenmeier, PPS-6, Annual Meeting, Nice (1990)
29) K.Funatsu, S.Kihara, M.Miyazaki, S.Katsuki, T.Kajiwara, *Polym. Eng.& Sci.,* **42** (4), p707 (2002)
30) H.Tomiyama, Y.Fukuzawa, JSW Technical Report, **67 (**11), p26 (2016)
31) K.Hirata, H.Ishida, M.Hiragohri, Y.Nakayama, T.Kajiwara, *Int. Polym. Proc.,* **28,** p368 (2013)
32) Y.Nakayama, E.Takeda, T.Shigeishi, H.Tomiyama, T.Kajiwara, *Chem. Eng. Sci.,* **66,** p103 (2011)
33) A.Gaspar-Cunha, J.A.Covas, B.Verges, *Polym. Eng. & Sci.,* **45,** DOI 10.1002, p1159 (2005)
34) H.Tomiyama, Y.Fukuzawa, D.Fukuzawa, *Seikei-Kakou*, **30** (4), p162 (2018)
35) B.Vergnes, *Int. Polym. Proc.,* **34** (5), p482 (2019)
36) T.Domenech, B.Vergnes, *et al.*, *Int. Polym. Proc.,* **27** (5) p517 (2012)
37) W.Lertwimolnun, B.Vergnes, *Polym. Eng. & Sci.,* **46,** p315 (2006)
38) J.W.Cho, D.R.Paul, *Polymer,* **42**, p1083 ( 2001)
39) N.Hasegawa. Y.Usuki, *et al.*, *Polymer ,* **44**, p2933 ( 2003) ]
40) H.Takase, H.Masago, Y.Katami, *et al.*, *Seikei-Kakou*, **16** ( 9), p616 ( 2004)
41) M.Kato,M.Matsushita, K.Fukumori, *Polym. Eng.& Sci.,* **44 (**7), p1205 (2004)
42) D.Litchfield, Q,Nguyen, D.Baird, SPE-ANTEC 2007, p72 (2007)
43) H.Takase, M.Furukawa, K.Kishi, J.Murakami, *Seikei-Kakou*, **14** ( 2), p126 ( 2002)
44) H.Takase, M.Furukawa, J.Murakami, *Seikei-Kakou*, **17,** p50 (2005)
45) C.Manus, SPE-ANTEC 2017 ( Anaheim), ( 2017)

46) O.Sidney, S.Carson, J.M.Maia, SPE-ANTEC 2016, p750 (2016)
47) H.Chen, V.Pandey, S.Carson, J.M.Maia, *Int. Polym. Proc.,* **35** (1), p37 (2020)
48) K.Matsumoto, T.Morita, Y.Arao, T.Tanaka, SPE-ANTEC 2019, ( 2019)
49) M.Matta, P.Anderson, SPE-ANTEC 2013, p1106 ( 2013)
50) H.H.Le, M.Tiwari, S.Ilisch, H.J.Radusch, 12th Symposium Polymer Blends, March ( 2007)
51) J.H.Radusch, *Plastics Age*, **57** (12), p78 (2011) and **58** (1), p74 (2012)
52) R.Dou, Y.Shao, S.Li, B.Yin, M.Yang, *Polymer,* **83,** p34 ( 2016)
53) T.Morishita, Y.Katagiri, T.Matsunaga, K.Fukumori, *Composi. Sci.& Techn.,* **142,** p41 (2017)
54) S.Kobayashi, *Plastics Age,* **60** (3), p100 (2014)
55) S.Kobayashi, *Plastics Age*, **60** (4), p116 (2014)
56) S.Kobayashi, *Seikei-Kakou,* **27** ( 4), p130 ( 2015)
57) Toyota Boshoku and Toyota Central R&D Labs. News Release, November 15, 2013
58) Precise Macromolecule NEDO Research Report (Sept. 2008)
59) K.Fukumori, et al., Toyota RD Report , **38** (1), p39 ( 2003)
60) M.Meysami, C.Tzoganakis, SPE ANTEC 2009, p640 (2009)
61) N.Lopattananon, T.Sakai, et al , *Int. Polym. Proc.,* **29** (3), p332 (2014)
62) N.Lopattananon, T.Sakai, et al , *Vinyl. Addit. Techn.* DOI 10 1002, p134 (2015)
63) N.Lopattananon, A.Walong, T.Sakai, *J. Appl. Poly. Sci,* DOI 10.1002, p46231 (2018)
64) T.Sakai, N.Lopattananon, PPS-35 Annual Meeting ( Turkey), June , ( 2019)
65) S.Ray, S.Pouliot, M.Bousmina, L.A. Utracki, *Polymer* , **45** , p8403 ( 2004)
66) A.Masa, R.Saito, H.Saito, T.Sakai, N.Lopattananon, *J. Appl. Poly. Sci.,* **133** (10), p43214 (2016)
67) S.Zhao, B.Xu, H.Yu, L.He, M.Wang, SPE-ANTEC 2016 , ( 2016)
68) H.Y.Lin, F.Q.Chen, R.B.Guo, G.Zhang, *Polym. Eng.& Sci.***35** (9), p829 (2015)
69) S.Jia, J.Qu, W.Liu, C.Wu, R.Chen, S.Zhai, Z.Huang, *Polym. Eng.& Sci.* DOI 10.1002, p716 (2014)
70) T.Sakai, *Plastics Age*, **62** (6) p45 (2016)
71) M.Erdermann, Ring Extruder Document: CPM Extrusion Group, ( 2019)
72) J.E.Loukus, A.Halonen, M.Gupta, SPE ANTEC 2004, p133 ( 2004)